HYDROLOGICAL EFFECTS OF INTAKE STOPS

by

Jessica van den Oort

A thesis submitted in partial fulfillment of the requirements for the degree of Master of Science in Earth, Life and Climate

Department of Geosciences

University of Utrecht

Super vision at KWR Water Cycle Research Institute by;

- Ir. M.L. van der Schans
- Dr.ir. D.G. Cirkel

Super vision at the University of Utrecht by;

- Dr. A. Raoof

Date of Approval:

August 15, 2016

Keywords: air, compression, entrapment, infiltration, column, experiment.

ABSTRACT

The phenomenon of compressed air upon infiltration in an unsaturated zone is a well-known problem. For water companies producing drinking water from infiltrated surface water in the dunes this phenomenon can seriously hamper production due to initially low infiltration rates after the system restarts. For this MSc thesis five experiments are conducted to study the effect of air confining and air draining conditions on the infiltration rate. In the first experiment the saturated conductivity of the soil column was determined. In the second and fourth experiment water was infiltrated by increasing the water table from the bottom up, venting air freely from the top of the column. In the third and fifth experiment, water was supplied at the top of the column resulting in entrapment of air between the wetting front and the saturated zone at the bottom of the column. Results show a short lived effect of compressed air in the first 4.7 minutes of experiment V. A limited effect is seen between the air-confined and unconfined infiltration rates (0.98) for experiment set IV and V. The air is not effectively retained due to escape of air along the column wall and due to air bubbles erupting through the wetting front. This is attributed to the small length of the column, by which in comparison the capillary is relatively high. Therefore, the difference in soil moisture values between the top of the column and water table are quite low (10%).

ACKNOWLEDGEMENTS

I would like to thank Dr.Ir. Gijsbert Cirkel and Ir. Martin van der Schans for supervising me and teaching me to design a column experiment and to think critically. From the University of Utrecht, I would like to thank my supervisor Dr. Amir Raoof for fruitful discussions and guidance. Thank you to Harry van der Wegen and Sydney Meijering whom have constructed the column and helped me during the experiments. I would like to express my gratitude to Prof. Dr.Ir Rien van Genuchten, Dr. Nobuo Toride and Dr. Mojtaba Mahmoodlu as well, for their thoughts on column experiment design.

List of figures

List of tables

Table of Contents

1 INTRODUCTION

1.1 Background

Along the Dutch coast the water companies Dunea, Waternet, PWN and Evides infiltrate water from the Rhine and Meuse rivers in the dunes, which is then filtered by movement through the sand and pumped or drained to be used as drinking water. The dunes serve as an artificial recharge system, in which aquifers are replenished by adding water through human effort. The water is added to prevent depletion of the aquifer through pumping of water for drinking water purposes. Dunea infiltrates water from the 'Afgedamde Maas' (a side branch of the river 'Meuse') at the areas Meijendel, Solleveld and Berkheide. PWN takes in water from the 'IJsselmeer' and infiltrates it at the dune area of Castricum. Waternet takes in water from the 'Lek canal' and transports it to the dune infiltration area Leiduin. Evides takes in water from the 'Haringvliet' for infiltration at Ouddorp.

Recently, the intake of river water for the artificial recharge system in the dunes ceased several times. The most important causes for these intake stops are a decrease in water quality (enhanced levels of micro pollutants), high chloride levels, air bubbles in water transportation pipelines, rupture of pipelines, low water level in infiltration ponds or maintenance. Examples of maintenance are the cleaning of pipelines from clogging substances, or clearing the ponds from dirt that has accumulated over the years. Besides maintenance, all of the above mentioned causes, are considered unexpected intake stops. Expected intake stops cause problems less frequently than expected intake stops, as water companies are able to anticipate just before the intake stop. For example, during an expected intake stop a water company can anticipate by taking in extra water prior to the start of the intake stop.

The frequency of unexpected intake stops will rise in the future due to climate change and the presence of new organic micro-pollutants (emerging substances). Examples of emerging substances are hormone disruptors, prescription drugs and their derivatives. The use of these emerging substances will rise as the average age of the Dutch population rises. The majority of the emerging substances is removed in sewage treatment plants, but part of it will still make its ways into the intake water of drinking water producing companies (Kools et al, 2007). Additionally, the climate change causes more fluctuation in discharge of the rivers Meuse and Rhine. In the summer and autumn the river will have less discharge due to drier periods, and in the winter and spring there will be more discharge. Less discharge results in higher concentrations of pollutants. If the concentrations found in the intake water are too high an intake stop can occur.

During intake stops, the water level in the ponds decrease as well as the water table and an unsaturated zone under the infiltration pond is able to develop. It is thought that the unsaturated zone allows for air to become entrapped by which the hydraulic conductivity is reduced. This effect results in a reduced infiltration rate, which causes the time to fill up the area underneath the infiltration pond to be longer than expected. The duration of filling up the unsaturated zone is essential to know for water companies, as lots of vegetation in the wet dune valleys surrounding the infiltration pond, depend on the soil moisture available. The severity of the reduction of the infiltration rate after an intake stop is illustrated by the following event. At Dunea, an intake stop took place (to clean the ponds) at the beginning of 2015. In February 2015, water was transported into the infiltration area again. It was expected that the groundwater level would be at target level again at the beginning of March. However, at the end of May 2015, groundwater level was still 0.75 m under target level.

The study presented in this thesis is part of the DPWE project at KWR. In the DPWE framework four (dune) drinking water producing companies (Dunea, PWN, Waternet and Evides) work together to obtain more specific knowledge about hydrological, hydro-geochemical and ecological effects of intake stops.

The aim of this thesis is to assess the effect of air entrapment on the outflow flux by conducting a column experiment. The research question is how the flux during unsaturated conditions changes when the air residing in the column is free to escape in comparison to when it is confined between the wetting front and artificial water table. Also, the effects of hydrological properties of the sand and boundary conditions used are discussed. The effect of air entrapment has been assessed in several studies before. However, only a few of these studies (Grismer, 1994) have performed a column experiment with a fixed head at the bottom of the column (the lower 10.0 cm of the column are saturated).

Secondly, the sand column is filled up at the bottom with water, controlled by a constant flux boundary condition. This condition turns into a constant head boundary, as soon as the pressure difference is 12.0 cm. The upper boundary of the column will act as a seepage face (experiment II). The third step is to apply a constant flux at the top of the column, which attains a constant pressure difference of 12.0 cm (experiment III). The lower boundary condition is a fixed head of 10.0 cm. Again, the soil moisture content, matric potential, and outflow will be measured.

It is expected that the outflow of the experiment with inflow at the bottom of the column results in a higher outflow, as flow of air is not impeded by a water table. Comparing the outflow of both experiments would thus provide information about the effect of air entrapment. The experiments I and II, will be repeated in experiment IV and V, but with a pressure difference of 62.0 cm to observe the effect of a higher pressure difference. The results of this column experiment will be modelled into Hydrus 1D, for further understanding of the results of the column experiment.

1.2 Objectives and scope

In this research the effect of air entrapment on outflow will be assessed by means of a column experiment. We hope to see a reduction in the infiltration rate during confining conditions, compared to air draining conditions. At infiltration ponds, the water table underneath the pond receives percolating water, and transports it to areas with a lower total head. The aim is to replicate this natural situation by artificially raising the water table (air draining) and compare it to ponded infiltration applied at the top of the column. The results will not be compared to field experiments but they will be modelled into the 1-dimensional Hydrus program. In Hydrus-1D air is able to escape during air confining conditions and thus makes comparison to experimental confining conditions possible.

2 REVIEW OF EXISTING LITERATURE

In this review existing literature about air entrapment and compressed air ahead of the wetting front will be discussed. Firstly, a process description of entrapped air will be given and then for compressed air. The main focus in the review will be on compressed air. The factors influencing the occurrence of compressed air will be discussed as well as under which conditions compressed air is released in regards of wetting front instability. Lastly, studies comparing air confining and air draining conditions will be discussed.

Before starting the literature review a few terms need to be clarified. In the literature there is confusion about *compressed air* and *entrapped air*. Air compression is air being compressed ahead of the wetting front, whereas entrapped air is air surrounded by water in the porous space of soils (Faybishenko, 1995).

Air draining and *air confining* conditions. During *air draining* conditions air is able to escape when the wetting front is moving downwards. The air will escape through an open bottom in the column or through open valves. Air confining conditions on the other hand, are conditions in which the air will be trapped between the wetting front and an (air-)impermeable layer (such as a clay layer), a water table, or a closed bottom in the column experiment.

Quasi saturated soils. Classically, the saturated zone is below the water table and the unsaturated zone lies above the water table. However, when air becomes entrapped beneath the water table the porous medium, is no longer saturated. Faybishenko (1995) introduced the term quasi-saturated zones for zones below the water table with entrapped air. In 1973 Vachaud et al, introduced a term for the conductivity and soil moisture content near saturation; K_0 and θ_0, respectively. This is the value for hydraulic conductivity and soil moisture content when the air content in the soil is at its minimal value (thus quasi-saturated). Since, it is hard to determine whether the soil is fully saturated, K_0 and θ_0 are adopted as symbols to indicate the soil moisture and hydraulic conductivity at residual air content. Additionally, when a soil is considered saturated, the soil moisture content will be at residual air content.

2.1 Air entrapment

2.1.1 Mechanism air entrapment

Air entrapment is the process in which air bubbles or small air pockets are being isolated from the rest of the soil matrix by the forward moving wetting front. This can occur for example for larger pores, in which the suction force is much smaller than in small pores, thus they may be skipped during infiltration. Vachaud et al. (1973) showed that the maximum soil moisture content behind the wetting front did not correspond with the porosity of the soil, so air must be entrapped. For air draining conditions the maximum soil moisture, θ_0, was about 0.34 $cm^3.cm^{-3}$, and approximately 0.32 $cm^3.cm^{-3}$ for air confining conditions, whereas the porosity is 0.42. Wilson and Luthin (1963) found that at higher air pressure the flow will mostly go through the smaller pores, and if infiltration is prolonged some of the air filled larger pores may be bypassed by the water and create dead end pores. This tells that if infiltration is not slow enough, it is likely for air to be trapped behind the wetting front, regardless of air confining or air draining conditions.

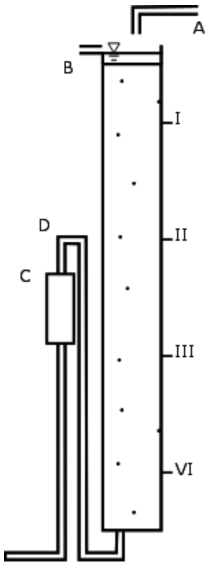

Figure 2-1 Set up of the experiment conducted by Lindenbergh (1941).

Lindenbergh (1941) (Figure 2-1) shows the effect of entrapped air on the hydraulic conductivity, even though the goal of this experiment was to determine the hydraulic conductivity of a soil in a column experiment by exerting different pressure gradients. In the first experiment the column was saturated by infiltrating water at the top of the column. In this experiment still 2.5% of air remained in the soil, and the hydraulic conductivity was 11.0 $m.d^{-1}$. In the second experiment, air was almost completely removed from the soil and the average hydraulic conductivity rose to 16.7 $m.d^{-1}$. Thus, entrapped air can have a great influence on the hydraulic conductivity at low residual air contents.

Faybishenko (1995) tried four different procedures to saturate in situ sampled cores: (1) saturation of the core by applying ponded filtration at the top of the core, (2) by mimicking a groundwater level rise in the column, (3) removal of air by placing the core in a vacuum chamber and then mimicking a groundwater level rise, (4) Degassing of the column with CO_2 and subsequently ponded infiltration. The first procedure resulted in entrapped air of 5 to 10 %, the second procedure had still about 5% entrapped air, and procedure 3 and 4 had about 0.1 to 0.2% entrapped air.

In the experiments by Faybishenko (1995) the hydraulic conductivity initially decreases during infiltration at the top of the column. The author suggested that the largest pores are being blocked by entrapped air. Although, air is initially locked in the smallest pores, by capillary forces the air is drawn out of the smaller pores (which are filled with water first) and the air is displaced into the larger pores.

The experiments done by Lindenbergh (1941), Vachaud et al. (1973), and Faybishenko (1995) show that mimicking a groundwater level rise results in a higher saturation of soil columns, whereas infiltration at the top of the column can lead to entrapped air percentages up to 10%. Also, air confining or air draining conditions differ in the amount of air being entrapped (higher for air confining conditions). The experiment by Faybishenko (1995) also shows the persistence of entrapped air and that hydraulic conductivity is usually not at its true value, even though the flux appears to be constant a few hours after initiation of the experiment.

2.1.2 Mechanism entrapped air removal

The removal of entrapped air is a slow process which can take up to 40 days (Faybishenko, 1995). The author divided entrapped air into mobile bubbles of air and immobile air that is captured in dead end pores. In the initial stages of entrapped air removal, mostly the mobile air will be released first by moving with the water flow. In this process the hydraulic conductivity will increase most, as said before, the larger pores contain most of the mobile air bubbles. The hydraulic conductivity increases because more pore space becomes available for the water to flow through.

The removal of immobile air can take up to 5 to 30 days, depending on the depth in the soil profile. Immobile air can only be removed by dissolution or consumption by bacteria. Temperature and pressure in the column can affect the dissolution of immobile air.

In the experiment by Faybishenko (1995) it was found that the hydraulic conductivity deeper in the column needed more time to recover to the hydraulic conductivity at saturation. The authors do not give a clear reason for this phenomenon, although it is said that microorganisms in the top of the soil column consume oxygen in the immobile air bubbles and release CO_2. CO_2 is known to dissolve more easily into water and thereby migrates downwards along with the infiltrating water. Entrapped air bubbles close the surface of the sand column can also escape more easily. It is not needed for the air bubbles to overcome the pore air entry pressure as the surface layer of the sand has a low shear strength. The pressure of the encapsulated air can mechanically push up the soil and create blowholes. The air then escapes from the surface, and the blowholes are filled with water.

The dissolution of air bubbles is dependent on the matric potential of the soil. During infiltration of water the matric potential of the soil increases (towards less negative values), and as a consequence the pressure inside the encapsulated air increases. When the matric potential is almost zero, large pressures develop in the entrapped air, as there is less and less space for the air (however, the pressure of the air behind the wetting front does not contribute to the total potential of the soil). When the pressure inside the air bubbles is larger than the atmospheric pressure, escape of the air bubbles is possible. The release of air bubbles allows for the infiltration rate to recover slowly, as more space will be available for the water. Complete removal of mobile and immobile air can result in a hydraulic conductivity being 10 to 40 times higher (Faybishenko, 1995).

2.2 Process description compressed air

In the first confined column experiments studying infiltration of water, it was thought that air could escape freely from the soil during infiltration and that the air pressure in the matrix would be similar to atmospheric pressure during air confining as well as air draining conditions. However, infiltration of water into the unsaturated zone is not a single phase process, it consists of two almost immiscible phases; water and air. When water infiltrates into the vadose zone, air may become compressed as the percolating water leaves less space for air. Depending on the boundary condition at the bottom and sides of the medium there is a chance for air compression to occur. When a water table is present, a closed column bottom or a soil layer with a low hydraulic conductivity (such as clay) air will be impeded to escape from the bottom of the column.

The air is only able to escape if it is capable to break through the wetting front or through the soil layer with a low hydraulic conductivity. If the air is not capable to break through the infiltration rate of water will drop significantly, possibly to zero. This is due to air pressure of the compressed air being so high, that water is unable to enter the pores at a high rate. There have been several studies showing a decrease in infiltration rate due to compression of air (Wilson and Luthin, 1963; Peck, 1965; Adrian and Franzini; 1966; Latifi et., 1994; Faybishenko, 1995). Another effect of higher air pressures near the wetting front is a lower soil moisture content due to water migrating to lower pressure areas (Wilson and Luthin, 1963).

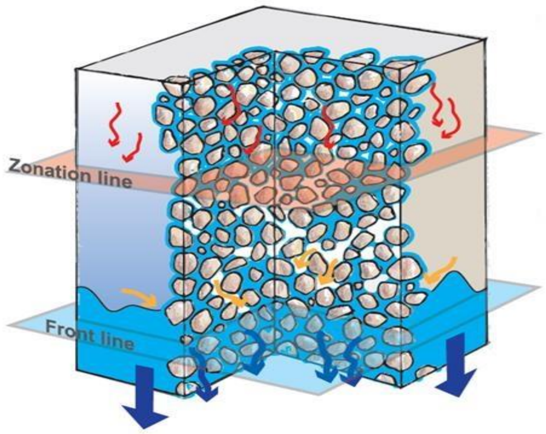

Figure 2-2. Infiltration of water into a soil. Red arrows depict the infiltrating water and yellow arrows the air. It is seen that air becomes stuck beneath the wetting front. The zonation line is the point at which the wetting front is and the front line is where the water table is found (figure modified from Or. et al (2012).

In unconfined experiments, the air pressure at the wetting front also increases. When the air pressure near the wetting front increases, the total head difference between the bottom and top of the column decreases. The decreased total head diminishes the hydraulic gradient and causes the water to infiltrate slower. In a study by Collis-George and Bond (1981) in most of the depth profiles the matric potential was -60 cm just before the wetting front reached the tensiometer. In addition the pressure of the air rose by 13 cm at maximum air pressure, which leaves a matric potential of -60 cm + 13 = -47 cm. However, as the air pressure just ahead of the wetting front decreased with time, the total potential gradient increased again with time, enhancing the infiltration rate eventually. The air pressure at the wetting front diminished over time as the air flowed out at the bottom of the column.

Collis-George and Bond (1981) described the process of compression of air ahead of the wetting front in unconfined experiments in detail. In their experiment water was applied at the top of the column and the bottom of the column was open to the atmosphere. At first the infiltration rate rises fast, resulting in large air displacement. In order to displace the large amount of air, the air pressure must rise as well ahead of the wetting front. And to produce the increase of air pressure, the air must be compressed. It takes time to build up enough pressure at the wetting front to displace the air, thus the air pressure and flux of air ahead of the wetting front do not reach a maximum instantaneously. Therefore, for some time the infiltration rate is decreasing while air pressure and the air flux are increasing. When the flux of air and flux of infiltration both reached the same value, the air pressure will be at its maximum.

2.2.1 Release of entrapped and compressed air.

When, the pressure of the air underneath the wetting front exceeds the air entry pressure of the soil, air will bubble through the wetting front and ponding layer. This can result in two effects. The first effect is drainage of the upper part of the soil as the capillary pressure is diminished during air bubbling. And (2), the escape of air bubbles may change the soil structure in the upper part of the soil, as the air bubbles air being pushed out mechanically.

2.2.2 Factors influencing air compression

There are a variety of factors influencing the likeliness of air compression, and the magnitude of air compression;

- The *(fluid) permeability* affects the velocity at which the water moves through the soil. If the permeability is high, then velocity is high as well, which can result in a faster compression of the air residing between the wetting front and the barrier.

- The *initial soil moisture content* of the soil has influence on the possibility for air compression to occur. If the amount of water in the soil is already high before infiltration begins, the effect of air compression will be small as there is limited space for air due to the high soil moisture content. Additionally, there is a great difference between an initial dry sand column and an initially drained column during air draining conditions. Wang et al (1998) observed air pressures to be close to atmospheric pressure and equal throughout the space under the wetting front. In comparison during air draining conditions with an initially drained column, the air pressure rose most (30 cm) just below the wetting front and the least at the bottom of the column (5 cm). The water at the bottom of the column prevented air from flowing into the pores.

- The magnitude of the flux imposed on the surface of the soil is of importance as well. Wakil (1972) found that with a flux rate of 2 $cm.h^{-1}$ and a soil moisture content of 0.29 $cm^3.cm^{-3}$, the air under the wetting front was not compressed. At this soil moisture content, air was still able to escape at the surface of the column. However, when the flux increased to 3 $cm.h^{-1}$, air was compressed beneath wetting front.

- *Column length*. The length of the column has influence on the ability of the soil column to retain compressed air during air-confining conditions. It seems that for shorter columns, the cumulative infiltration and air pressure are more likely to attain equilibrium, than for longer columns. In the longer columns the cumulative infiltration rate keeps increasing as well as the air pressure. For example if water in a soil column with a length of 80 cm infiltrates 10 cm (and no air escape), the reduction in available space for the air is; 10/80 = 0.125. To achieve the same reduction in available space in column of 100 cm, the water would have to infiltrate; 100 * 0.125 = 12.5 cm. Thus, in the longer soil column the cumulative infiltration rate will be larger. It is not though not known why air pressure can keep rising to higher values than in the shorter column, although it can be argued that in the longer column the pressure of the overlying water is higher due to larger wetting front depth. The depth of the wetting front and the air entry pressure together determine if air will break through the wetting front. In the column experiment from Peck (1964, 1965) the influence of column length was shown. It was seen that for a column length of 133 and 322 cm no air escaped from the column. The cumulative infiltration rate stopped increasing after 5 and 10 minutes respectively as well as the pore air pressure. The author conducted the same experiment on longer columns (410 and 490 cm). In these columns, for air-confining conditions, cumulative infiltration rose throughout the experiment, but the air started to escape after about 40 minutes as pore air pressure diminished and the cumulative infiltration rose.

- *Pore size.* Adrian and Franzini (1966) discussed the effect of pore size in air draining and air confining experiments. For their experiment three different materials were tested; uniform glass beads of 0.08 mm diameter, graded glass beads with a varying size of 0.03 to 4 mm (geometric mean of 0.123 mm) and a Roseville white sand with a geometric mean of 0.305 mm. In the uniform glass beads of 0.08 mm, it was found that during air confining conditions, the infiltration rate decreased exponentially with time, from 43.20 $m.d^{-1}$ after 25 seconds to 1.73 $m.d^{-1}$ after 180 seconds, to 0.00 $m.d^{-1}$ after 350 seconds. In comparison, the Roseville white sand the infiltration rate also decreases exponentially, however, it does not approach zero but it attains the saturated hydraulic conductivity value. Smaller grainsize is related to a smaller pore size. Thus, the smaller the pore size, the more likely it will be that the air will be compressed and infiltration will cease due to the pressure of the air.

- *Homogeneity of the soil*. The pore size also has an effect on infiltration. The authors saw that in the experiments with the graded glass beads that the wetting front was less sharp than for uniform glass beads or the Roseville white sand. The range in grainsize leads to a range in pore sizes, all with different suction values. Thus, the smaller pores are filled first and then the larger ones, which can cause an uneven propagation of the wetting front.

- *Wetting front instability.* The infiltration of water during air confining conditions can affect the wetting front in such a way that it becomes unstable, whereby fingers are being formed. Fingers are preferential flow paths for water. The formation of fingers can cause the earlier arrival of a flux at the bottom of the column. Preferential flow in soil columns can affect the wetting front in soil columns in such a way that the wetting front becomes unstable. Especially in soils with a varying grainsize the wetting front can easily become unstable. Wang et al. (1998) recorded the depth of the wetting front during air draining and air confining conditions (figure 2-2). The most notable differences are that the wetting front during air draining conditions moves almost as a straight line downwards, and with a higher velocity. During air confining conditions the wetting front becomes more and more irregular with time and areas with fingers have farther spaced isolines. There most of the flow occurs and not in the areas with the isolines close together. The irregularity in isolines means that there are different flow velocities inside the column, thus the outflow will be the mean of these velocities.

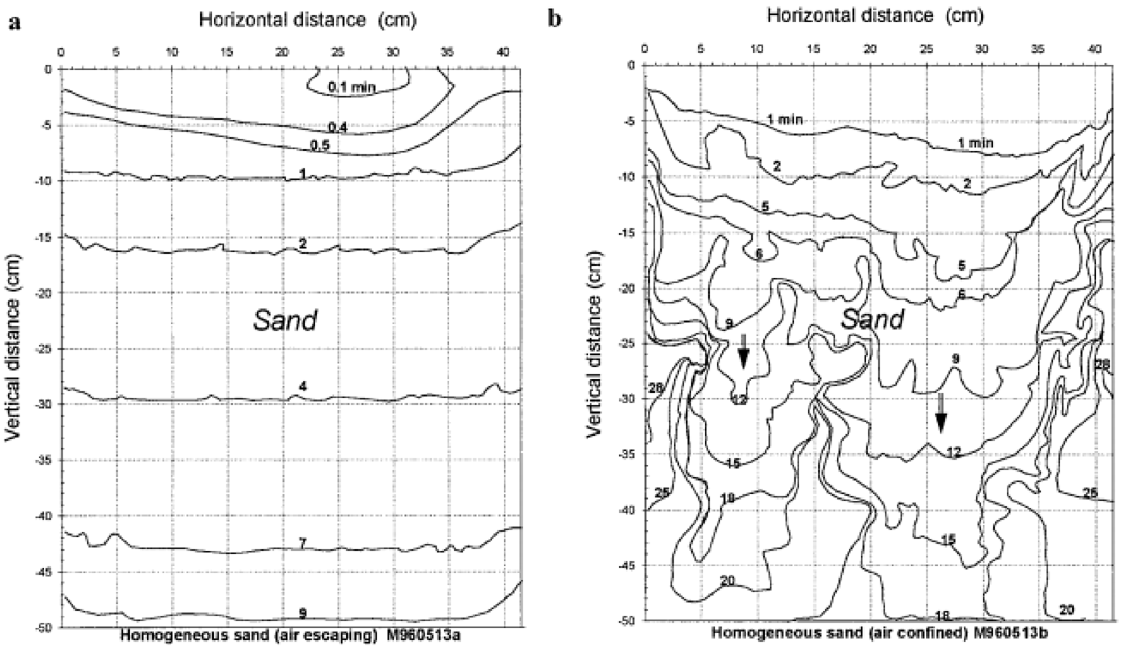

Figure 2-3. Propagation of the wetting front during air draining conditions (a, left figure) and during air confining conditions (b, right figure) from Wang et al. (1998).

The infiltration rate and air pressure seem to try to obtain a balance. Usually, the infiltration rate is very high at first and the air pressure low, but then the situation is reversed. As the air pressure keeps increasing the infiltration rate gets lower and lower (Wilson and Luthin, 1963) until both become steady. The authors also suggested that fingers can start to form during infiltration, and that some of the areas between the fingers might become isolated as the wetting front advances. This in turn increases turn increases tortuosity of the flow, which lowers the infiltration rate.

2.3 Quantifying the effect of air compression

The effect of air compression can be quantified by comparing column experiments of air draining conditions to air confining conditions Peck (1964). The ratio is obtained by dividing the (cumulative) infiltration rate of the confined experiment by the (cumulative) infiltration rate of the unconfined experiment. During air draining conditions in a column experiment the air residing in the soil has enough space to escape downwards upon infiltration into the soil. In general it is found that infiltration into soil columns with air draining conditions do not affect the infiltration rate. When the soil column is confined, no air can escape through the bottom of the column when water is being infiltrated. For example if a soil in the field has a confining layer, such as a clay layer, air may be significantly compressed. In the following section, column experiments that been conducted to compare air confining conditions to the previously described air draining conditions are shortly described along with their results. Only Peck (1964) reported ratios between confined and unconfined infiltration rates, in other studies (Wilson and Luthin (1963), Franzini (1966) and Vachaud (1973)) ratios were derived from the data provided in the papers (Table 2-2). Not all ratios could be obtained at the same time after the start of the experiment as some experiments last a couple of hours (making the determination of (cumulative) infiltration at 5 minutes after the start of the experiment difficult in graph data) whereas others last only 20 minutes. It must be taken into account that a ratio after 2 minutes cannot be compared directly to a ratio after 5 minutes, as usually the effect of air compression becomes more evident the longer the experiment runs.

The studies by Wilson and Luthin (1963) and Vachaud (1973), no specific conditions (such as grainsize or column length) were tested. The ratios in these studies can give a general idea of how air draining and air confining conditions relate to one another. The cumulative infiltration rate in both studies diminishes by approximately 37 to 47% during air confining conditions.

Peck (1965) focused specifically on the influence of column length. The ratio between confined and unconfined infiltration is 0.10 for the 390.0 cm column, whereas it is 0.004 for the 133.0 cm column (Table 2-2). In the cumulative infiltration graph of the 133.0 cm column it is seen that infiltration stopped after 5 minutes. This means that water was essentially withheld from infiltrating as the infiltration rate was a factor of 250 lower than for the unbounded experiment. It emphasizes the influence of column length. There were also columns with a smaller length of 13.0, 100, and 200.0 cm used. However, the ratios for these columns cannot be compared to the 133.0 and 390.0 cm columns as a slate dust was used. Though, the ratios also confirm that with a smaller column length the ratio also becomes smaller. This means that air compression has a greater influence and that the infiltration rate in a confining experiment will approach zero sooner than in a longer column. For example in the 200.0 cm column the ratio is 0.55 and in the 100.0 cm column the ratio is 0.25 after 20 minutes.

In Vachaud et al. (1973), air draining conditions were achieved by having the bottom of the column open to the atmosphere and inserting hypodermic needles in the column to allow escape of air. The air confining conditions were achieved by putting rubber stoppers on the hypodermic needles and sealing the bottom of the column. At the start of the experiment the column was drained, after which water was allowed to infiltrate at the top of the column. During air draining conditions the air pressure inside the soil column, was similar to air pressure and no effect on the infiltration rate was seen. The pressure inside the column being similar to air pressure, means that no air compression occurred. For air confining conditions, it was observed that the advance of the wetting front was significantly slower as air is being compressed in a smaller and smaller pore space. Also, the time to reach the bottom of the column (transit time) was significantly longer (0.8 to 1 hour, in comparison to 0.5 to 0.6 hour for air draining conditions). The ratio between confined and unconfined cumulative infiltration changed slightly from 0.65 after 5 minutes to 0.63 after 1 hour. The cumulative infiltration effectively stopped after 1 hour, due to air pressure being too high for further infiltration. Then the ratio diminishes to 0.57 in only 7 minutes.

Wang et al. (1998) did report an air pressure increase of 30 cm upon infiltration in an air draining column. However, in this study air draining conditions were set by setting an artificial water table in a previously drained soil column and air was allowed to drain through one tube in the wall of the column. It could be that the air residing between the wetting front and the water table was discontinuous, meaning that air resided in multiple air pockets with preferential flow paths in between. If the valve does not connect with one of the air pockets inside the column, the column will become air confining. Additionally, a column with an open bottom (such as in Vachaud et al. 1973) has more surface area for the air to flow out in comparison to only installing a tube in the wall of the column. Therefore, it is more reliable to insert multiple hypodermic needles, in order to increase the likeliness of intersecting such an air pocket. Also, Wang et al. (1998) reported that air pressure difference between the wetting front and the water table caused water to flow out of the bottom of the column, instead of air erupting at the surface. In order to prevent water moving out of the soil column, the counteracting pressure of the water should overcome the pressure of the air.

Wang et al. (1998) reported effects of air compression during air confining conditions as well. They achieved air confining conditions by closing off the valve that allows for air escape. The soil was not pre-wetted as in the air draining case, it was completely dry. Now air pressure rose by 40 cm instead. Air erupted frequently at the top of the column, as the air entry pressure value was exceeded. This phenomenon directly increased the infiltration rate, which became lower again as the wetting front proceeded downwards. No ratio was determined for these experiments as the air draining column was previously water drained, whereas the air confining column was dry at the start of the experiment.

Grainsize must also be taken into consideration when assessing the effect of air compression. The study by Franzini unfortunately did not have data for unconfined flow in the Roseville white sand. However, it is notable that for the 0.08 mm grains, the infiltration rate drops from 19.74 $m.d^{-1}$ till 1.73 $m.d^{-1}$ for unconfined and then confined conditions. In the Roseville white sand it was found that the infiltration rate is 47.52 $m.d^{-1}$ during confined conditions. They also noted that for grainsizes larger than 0.3 mm, air can easily escape due to the low air entry pressure of the soil. The larger a grainsize is the lower the air entry pressure generally is. Konyai et al. (2009) determined the air and water entry of soils with a different grainsize (Table 2-1). More coarse soils have a lower air entry pressure than

Table 2-1 Air entry values for different D_{50} values (modified from Konyai et al. (2009)).D_{50} is the particle size at 10% of the cumulative distribution of a grainsize distribution of a particular soil

Soil	D_{50}	Air entry pressure
	[mm]	[cm]
Loam	0.035	9
Loamy Sand	0.130	20

Table 2-2 Comparison infiltration ratios for confined and unconfined infiltration.

	Author								
Variable	Wilson and Luthin (1963) (horizontal experiment)		Peck (1965)			Franzini (1966)		Vachaud	
Column dimensions	31.0 cm length, 4.5 cm I.D		133.0 cm length , 2.0 cm I.D	490.0 cm length, 2.0 cm I.D	(1) 200.0 cm length, 2.0 cm I.D (2) 100.0 cm length, 2.0 cm I.D	137.0 cm length, 4.45 x 6.35 cm rectangular column		56.0 cm length	
Material	Columbia silt loam		Air dry medium sand		Slate dust	Uniform glass beads	Roseville white sand	San	
Grainsize	-		0.25 to 0.50 mm (Wentworth, 1922)		0.0039 to 0.0078 mm (Wentworth, 1922)	0.080 mm	Geometric mean = 0.305 mm	0.8 to 0.0 with 50 %	
Porosity	Unknown		Unknown		Unknown	Unknown	0.47	0.42	
Boundary condition top	Constant pressure		Constant pressure		Constant pressure	Constant pressure		Constant p	
Boundary condition bottom	No flow boundary (air draining)	No flow boundary (air confining)	Free drainage		Free drainage	Closed bottom (confined), open bottom (unconfined)		No flow boundary, with air release	
K_0	Unknown		17.30 m/d		2.16 m/d	Unknown		Unkno	
Cumulative infiltration (A)/Infiltration rate (B)	(A) (5 min): 1.90 cm, (A) (10 min): 2.65 cm	(A) (5 min): 1.20 cm, (A) (10 min): 1.40 cm.	(A) Confined (30 min): 3.60 cm (A) Unconfined (30 min): 900 cm	(A) Confined (30 min): 8.96 cm, (A) Unconfined (30 min): 89.60 cm	(1) (A) confined (20 min): 2.51 cm (1) (A) unconfined (20 min) : 4.56 cm (2) (A) confined (20 min) : 2.23 cm (2) (A) unconfined (20 min) : 8.91 cm	(B) Unconfined (3 min): 19.74 m/d (B) Confined: (3 min) 1.73 m/d	(B) Unconfined: - (B) Confined: (3 min): 47.52 m/d	(A) Unconfined (5 min): 3.02 cm (A) Unconfined (1 h): 15.00 cm	
Ratio; Air confining/air draining	(A) ratio (5 min): 1.20/1.90 = 0.63, (A) ratio (10 min): 1.4/2.65 = 0.53		(A) ratio (30 min): 3.6/900 = 0.004	(A) ratio (30 min): 8.96/89.6 = 0.10	(A) ratio (1)(20 min): 2.51/4.56 = 0.55 (A) ratio (2) (20 min): 2.23/8.91 = 0.25	(B) ratio: 1.73/19.74 = 0.09	-	(A) ratio (5 min): (A) ratio (1 h): 9.0	

3 MATERIAL AND METHODS.

3.1.1 Description column

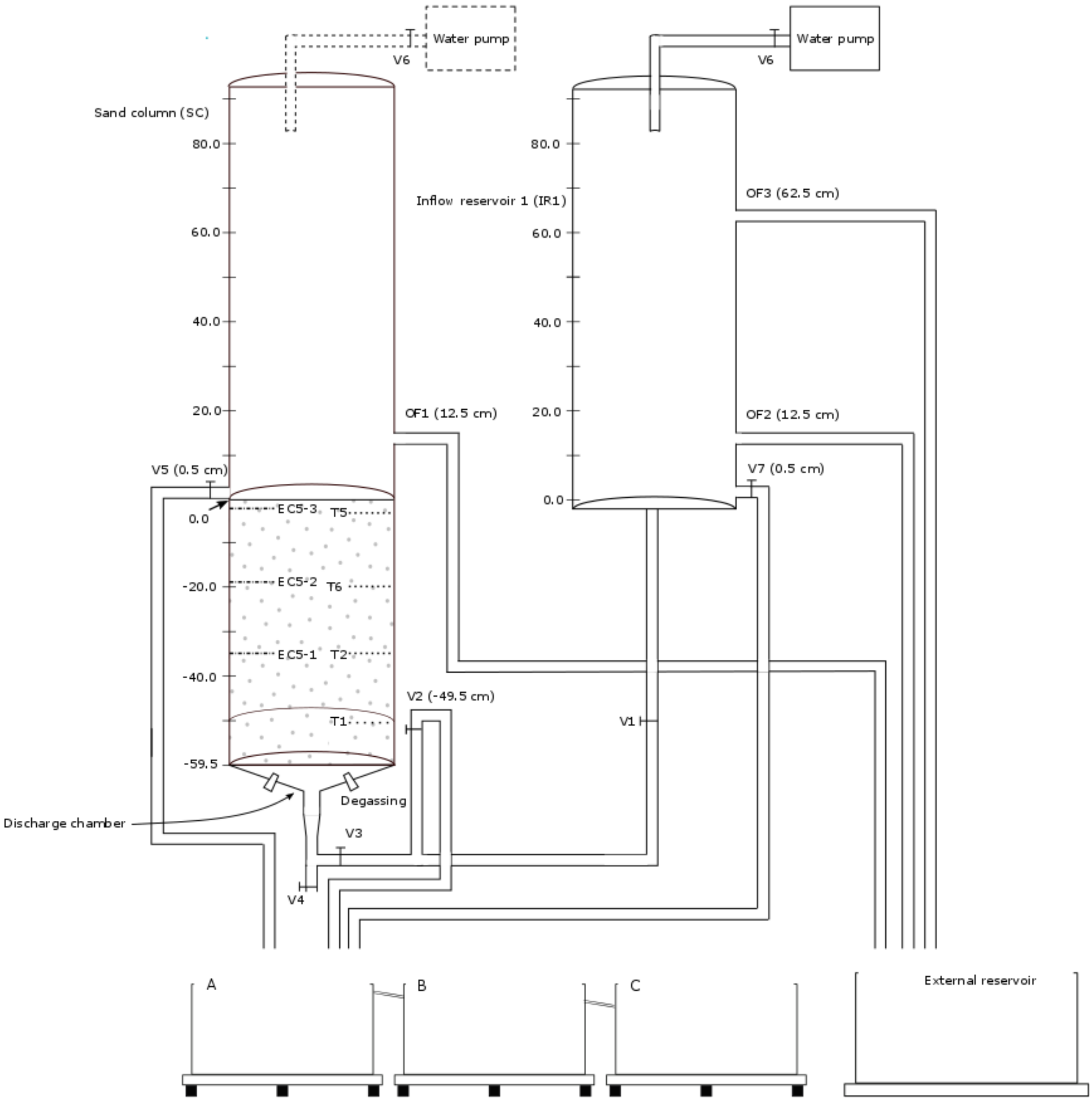

Figure 3-1. Schematic column set up.

In this experiment a 150 cm column made of PVC-U (Figure 3-1), with a diameter of 37 cm is used. The column is open to the atmosphere at the top and closed at the bottom by an artificial water table (fixed head). Ground level is at 0.0 cm, with negative values extending into the sand and positive values above the sand. The sand column is filled with air dried fine sand from -59.5 cm to 0.0 cm. At 0.0 cm there is a layer of 2.0 cm of glass pearls (0.3 cm diameter, and a density of 2550 kg m^{-3}) on top of the sand. The glass pearls spread water coming from the pump equally over the surface of the column and prevent disruption of the top sand layer due to the force of the falling water.

The tensiometers are inserted at height of -3.5 (T5), -20.0 (T6), -35.0 (T2) and -50.0 (T1) cm. The soil moisture sensors; EC5-1, EC5-2, and EC5-3 are inserted at a depth of; -35.0, -19.0, -2.5 cm. The sensors are connected to a data logger (CR1000) which in turn is connected to a computer. The bottom of the column has a raster with a 100 µm filter on top, which allows for the water to flow out, but retains the sand. Underneath the filter there is a discharge chamber. The discharge chamber has two small caps. One cap is to inject CO_2 into the discharge chamber and the other cap is for air to flow out of the discharge chamber and column during injection of CO_2. More details are given in section 0. During the experiment, when the column is being drained or when unsaturated infiltration occurs, the artificial water table is always kept at a height of -48.5 cm, meaning that the discharge chamber, 11 cm of the sand column height and tube area between V1, V2, and V4 is always filled with water. The 11 cm of saturated soil under the artificial water table is there to provide extra resistance to air pushing out water from underneath the water table when infiltrating at the top of the column.

Next to the soil column, there is an inflow reservoir (IR1) with a diameter of 37 cm. IR1 serves to supply water to the sand column by infiltration at the bottom (through the tube at V1 and V3) or it can serve as an outflow point when water is applied at the top of the sand column. Water is then discharged through V7 into container A, B or C. Valve V6 can supply tap water to both IR1, for bottom infiltration, as well as directly onto the sand column for top infiltration. In Figure 3-1 the tap is given as a solid line and as a dashed line. The dashed line gives the position of the tap when supplying water at the top of the sand column.

Under the discharge chamber there are three containers to collect water, outflow container A, B and C. A is connected to B and B is in turn connected to C. If measurements continue at night there is a fourth container, container D. Under each reservoir there is a scale that can measure a maximum weight of 12 kg. When A is full, excess water will flow into B. When B is full, excess water will flow into C. All scales together can measure a weight up to 36 kg. Container D is not connected to a scale, however with a diver in the container, an estimation of the flux (after A, B and C are filled) can still be made. Container D will only be used in the night, when the cumulative outflow will be too much for container A, B and C.

Under IR1 there is an external reservoir. In the external reservoir is used to collect excess water flowing from OF1 (Experiment III and V), OF2 (Experiment I and II) or OF3 (Experiment IV). The volume of overflow is estimated by measuring the height of the water in the external reservoir multiplied by the cross section of the reservoir. The external reservoir is also used to drain the ponding water layer in IR1 (by placing the flexible tube at V5 into the external reservoir) or the ponding water layer in the soil column (depending on the experiment). Another diver is placed in IR1 to measure the height of the water when infiltrating from the bottom. The same diver is placed on top of the soil column when infiltration occurs at the top of column.

3.2 General description experiment

A total number of 5 experiments will be conducted, in Table 11-1 the experiments are summarized. Firstly, the saturated flux is determined in experiment I. Then two sets of experiments are conducted to evaluate the effect of air entrapment. In the first set of experiments (Experiment II and Experiment III) the effect of air entrapment is assessed by firstly saturating the column from the bottom upwards and secondly saturating it from the top of the column downwards. Both setups are designed to have a total head difference of 12.0 cm. However, the total head difference of experiment II turns out to be 12.0 cm and in experiment III it is 12.5 cm. Prior to the start of experiment II, III, IV and V, the column is drained for about 3 days, 19 hours, 20 minutes and 47 seconds (3.81 days). The reason for choosing 3.81 days is because after this amount of time neither the matric potential nor soil moisture sensors in the Hydrus drainage model recorded any significant change. After drainage of the column, water is infiltrated at the bottom (Exp. II) or at the top (Exp. III) by applying a constant flux until the water height in the inflow reservoir IR1 is 12.5 cm (Exp.II) cm or 13.0 cm on top of the soil column (Exp. III) (Figure 3-1), then the boundary condition at the bottom is set at a constant pressure by letting excess water in IR1 or on top of the soil column flow into the external reservoir. The outflow is measured until a constant value is reached. In the second set of experiments (Experiment IV and V), the sand column is drained again for 3.81 days. In the initial design both experiments would have a total head difference of 62.5 cm, though precise measurement revealed a total head difference of 62.9 cm for experiment IV and 61.5 cm for experiment V. The total head difference for each experiment is reached by infiltrating at the bottom of the column in experiment IV and at the top in experiment V. The outflow is measured until a constant value is reached. The difference between the outflow experiment IV and V provides information on the effect of air entrapment on permeability. For a more detailed description see appendix 11.

3.2.1 Boundary conditions

In this section, the boundary conditions used in Experiments I to V and the drainage scenario is explained. The variable pressure head at the top or bottom of the column will be built up by a constant flux of about 103 $L.h^{-1}$, which is equal to 9.6 $cm.h^{-1}$. As the value for the constant flux will be higher than the maximum infiltration rate, water will build up in IR1 or on top of the column, until the water level has increased to the desired height (depending on the experiment) after it will overflow at OF1, OF2 or OF3. After reaching the overflow point the boundary condition will switch from a constant flux to a constant pressure. The outflow point (V5) is situated 0.5 cm above the soil surface. A space of 0.5 cm above the soil surface was thought to be handy as sand at the top of the column will not be able to enter the tube at V5. As the outflow point is 0.5 cm above the soil surface, the top boundary condition during bottom infiltration changes to a constant pressure of 0.5 cm when water has reached V5 (in Experiment I, II and IV).

Drainage of the column – In experiments II to V the column will be drained prior to the start of the experiment (Figure 3-2). The *lower boundary condition* is a fixed head of 11.0 cm. In practice this means that the tube underneath the column connects to V2, and the outflow at V2 is set at -48.5 cm. Thus, water infiltrating downwards will flow out at V2 when the pressure at the bottom of the column is equal or more than 11.0 cm and the bottom 11.0 cm of the column remains saturated. The upper boundary condition is an atmospheric boundary condition, as no water is infiltrated during the drainage process.

Experiment I – The *upper boundary condition* is an atmospheric boundary condition. This way the upwards infiltrating water can freely exit the column at V5. When outflow starts the pressure at the top of the column will be around 0.5 cm constantly, due to the fact that V5 is 0.5 cm above the top of the soil (Figure 3-3). The *lower boundary condition* is a variable pressure head until the water height in IR1 is at 12.5 cm. Then the lower boundary conditions will change into a constant head. The total head difference, at the end of the experiment, between the top and bottom of the column can be calculated as follows;

$$H_1 = h_1 + z_1$$ *Eq. 3-1*

$$H_2 = h_2 + z_2$$ *Eq. 3-2*

and,

$$H_2 - H_1 = \Delta H$$ *Eq. 3-3*

thus,

$$h_2 = \Delta H + h_1 + z_1 - z_2$$ *Eq. 3-4*

$$h_1 = h_2 - \Delta H - z_1 + z_2$$ *Eq. 3-5*

In which $H_{1,}$, z_1, and h_1 is the total head, depth and pressure head at the surface of the soil column and H_2 z_2, and h_2 is the total head, depth and pressure head at the bottom of the soil column. ΔH is the total head difference. For experiment I;

h_1 = 0.5 cm, z_1 = 0.0 cm, and h_2 = 72.0, z_2 = -59.5 cm, thus ΔH = (72.0 + -59.5) – (0.5 + 0.0) = 12.0 cm.

ΔH for experiment I is reached at the end of the experiment. At the start of the experiment ΔH is zero as the water level in IR1 is at 0.0 cm, just as in the soil column.

Experiment II – The upper boundary and lower boundary condition are similar for experiment I, only in this experiment the column is drained prior to the start (Figure 3-2). Figure 3-3 shows the situation at the end of the experiment.

Experiment III – Now, the flow direction is reversed as the water is infiltrated at the top of the column (Figure 3-4), thus *the upper boundary condition* is a variable pressure head until the ponding water reaches OF1 (at 12.5 cm height at the soil column). The bottom boundary condition will be a constant pressure head at the end of the experiment. The total head difference at the end of the experiment will be:

h_2 = 13.0 cm, z_2 = 0.0 cm, h_1 = 60.0 cm, and z_1 = -59.5 cm, thus ΔH = (13.0 + 0.0) – (60 + -59.5) = 12.5 cm.

Unfortunately, the total head difference is not the same in experiment II and III. This is caused by the fact that the overflow point OF1 was drilled at +13.0 cm height, and OF2 (in Exp II) was drilled at +12.5 cm). Though, the difference in the height of the outflow point can be corrected later on.

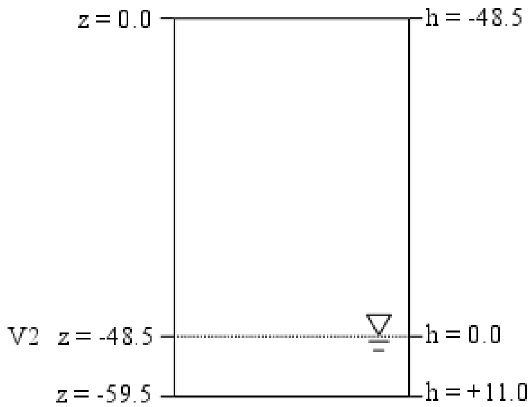

Figure 3-2 Matric potential values in the sand column after drainage (in cm)

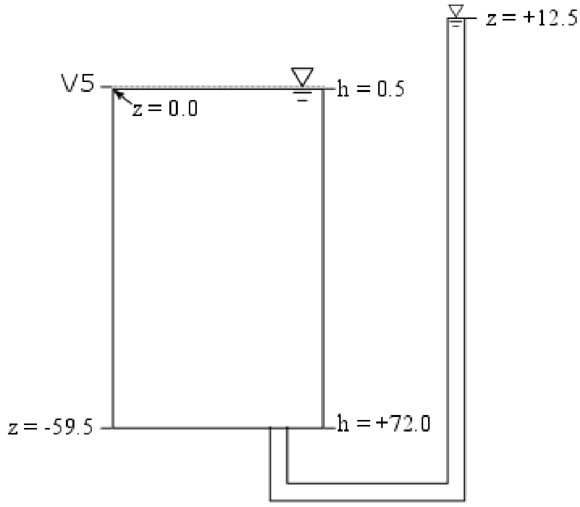

Figure 3-3 Matric potential values in the sand column after applying a constant pressure at the bottom of the column, with a pressure difference of 12.0 cm between the outflow point V5 (0.5 cm) and the top of the water level in IR1 (12.5 cm).

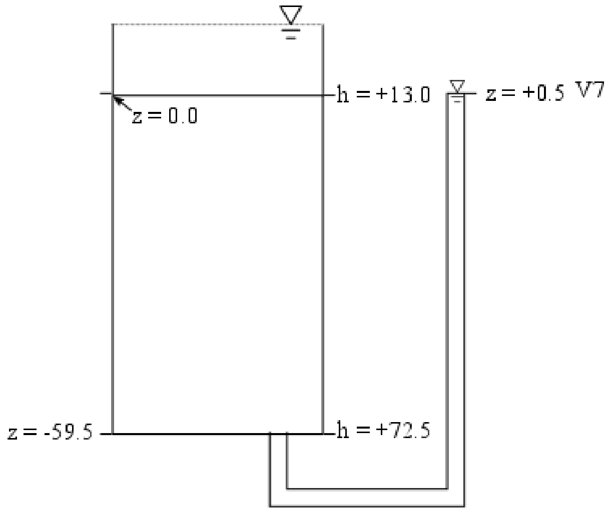

Figure 3-4 Application of water at the top of the column in experiment III. The total head difference between the outflow point (V7) and water level at the sand column is 12.5 cm.

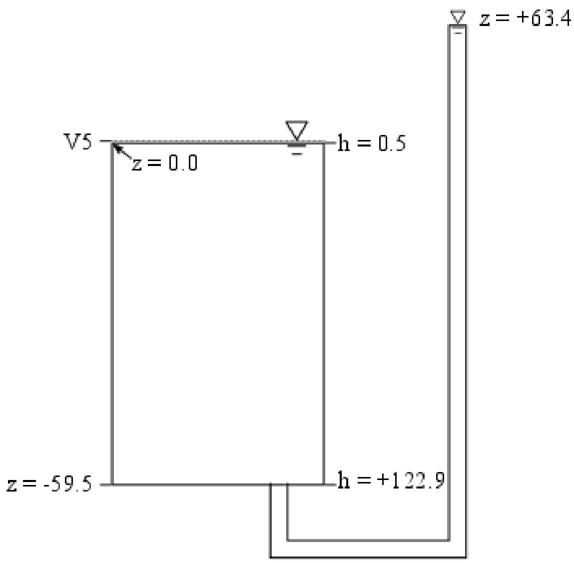

Figure 3-5 Bottom infiltration during a total head difference of 62.9 cm (exp. IV) between the top of the water level in IR1 (+63.4 cm) and the outflow point V5 (+0.5 cm)

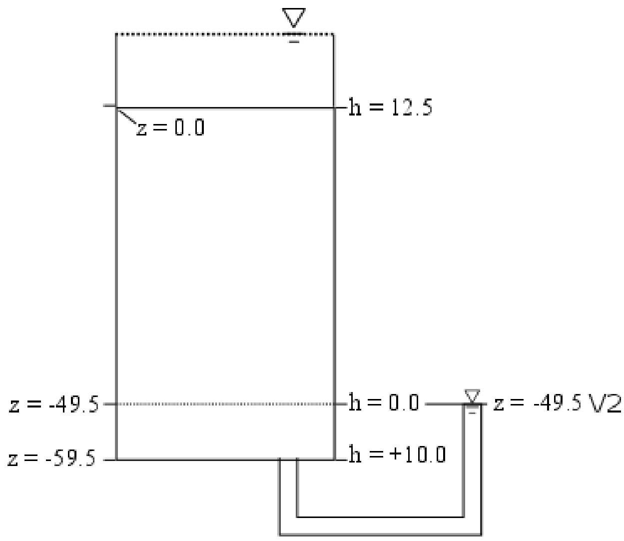

Figure 3-6 Experiment V, top infiltration during a pressure difference of 62.0 cm between the top of the water level on top of the column and the outflow point at V2.

Experiment IV – Water is infiltrated at the bottom of the column again (Figure 3-5), but with a larger total head difference. The *upper boundary condition* is an atmospheric boundary. *The lower boundary condition* is a variable pressure head at the start and at the end a constant head. The total head difference at the end of the experiment is;

h_1 = 0.5 cm, z_1 = 0.0 cm, h_2 = 122.9 and z_2 = -59.5 cm, thus ΔH = (122.9 + - 59.5) – (0.5 + 0.0) = 62.9 cm.

At the start of the experiment IV, the water level in IR1 is at 50.0 cm and is then increased to 63.4 cm.

Experiment V – In scenario V, the *upper boundary condition* is a variable pressure head and the *lower boundary condition* is a constant head of 11.0 cm (Figure 3-6). In this experiment V2 is opened for outflow instead of V5 in IR1. The pressure at the bottom of the column is 11.0 cm as the bottom 11.0 cm is always saturated. The total head difference is;

h_2 = 13.0 cm, z_2 = 0.0 cm, h_1 = 10.0 cm, and z_1 = -59.5 cm, thus ΔH = (13.0 + 0.0) – (11.0 + -59.5 = 61.5 cm.

When attaining steady matric potential profiles, the pressure at the bottom of the column is 11.0 cm and at the top it is 12.5 cm. Unfortunately, the total head difference between experiment IV and V is not similar, as the overflow point, OF3, was not drilled at the appropriate height (+63.0 cm, if the total head difference was 62.5 cm)) and outflow point V2 turned out to be at -48.5 cm instead of -49.5 cm. Table 3-1 summarize the height of the outflow or overflow points and Table 3-2 summarizes the total head difference and ponding height for each experiment.

Table 3-1 Checking the boundary conditions by comparing the depth to the water level for each outflow point.

	Height compared to reference level
	[cm]
V2	-48.5
V5	0.5
V7	0.5
OF1	13
OF2	12.5
OF3	63.4

Table 3-2 The calculated total head difference based on the water pressure applied at the bottom and top of the column for each experiment and the corresponding ponding height.SC stands for soil column.

Exp.	Total head difference	Ponding height
[#]	[cm]	[cm]
I	12.0	12.5 (IR1)
II	12.0	12.5 (IR1)
III	12.5	13.0 (SC)
IV	62.9	63.4 (IR1)
V	61.5	13.0 (SC)

3.3 Soil material and calibration sensors

3.3.1 Characterization soil material

The soil material for the column experiment was taken from the Meijendel dune infiltration area. A particle size analysis was performed with the Sympatec HELOS (H1408) apparatus (see Figure 10-1 in the appendix). This apparatus measures the grainsize of the sand with a laser. As the particles in the soil are not perfect spheres, the laser will sometimes measure the long diameter of the particle, which could result in overestimation of the average grainsize. The grainsize of the dune sand varies from 0.09 to 0.52 mm, with 50% of the particles having a grainsize lower than 0.23 mm.

According to the Wenthworth grain-size scale (Wentworth, 1922) for clastic sediments this sand can be classified as a fine to medium sand. The scale determines a grain-size of 0.063 to 0.125 mm to be very fine sand, 0.125 to 0.250 mm fine sand, 0.250 to 0.500 mm as medium sand and 0.500 to 1.000 mm is said to be coarse sand. In the particle size analysis about 2.5 % is of the soil particles is classified as very fine sand, 55.0 % is fine sand, 44.0 % is medium sand and less than 1.0 percent is categorized as coarse sand.

Porosity has been determined by saturating and subsequently drying out an in situ obtained core sample. This was done after all experiments had been conducted. The saturated weight was 197.39 g, dry weight 160.12 g and the volume of the sample is 100.14 cm^3. The weight of the water inside the soil sample was 197.39-160.12 = 37.27 g. As the density of water is 0.999997 $g.cm^{-3}$, the volume of water is 37.12 cm^3. Porosity is the volume of air divided by the total volume of the sample, thus porosity is: (37.27/100.14)*100 = 37.2 %. According to Domenico and Schwartz (1990), the hydraulic conductivity belonging to a soil with predominantly fine and medium size grains ranges from 9E-7 to 5E-4 $cm.s^{-1}$ for medium sand and from 2E-7 to 2E-4 $cm.s^{-1}$ for a fine sand. Converted into $cm.d^{-1}$ this is; 7.8 to 4320.0 $cm.d^{-1}$ for medium sand and 1.7 to 1728 $cm.d^{-1}$.

3.3.2 Soil moisture sensors

Calibration of the soil moisture sensors is necessary as the default calibration lines in the logger itself (CR1000) are not applicable for every type of soil. The soil moisture sensors were tested by inserting each sensor into a saturated soil sample, and subsequently drying it by exposure to the air. For each sensor a soil sample was prepared in the following way; a PVC (internal diameter (I.D) of 7.66 cm, and length of 10.0 cm) cylinder was packed with air dried dune sand. A cheesecloth was fixed at the bottom of the cylinder to allow for infiltration of water and prevention of sand slumping. The top of the cylinder was connected to the atmosphere. Each cylinder was then slowly saturated by placing the sample into a beaker glass filled with a layer of 1 cm of water. Each time step, the water layer in the beaker glass was increased by 1 cm. When the water level inside the beaker glass was as high as the top of the soil in the cylinder, the samples remained submerged for another day to increase saturation prior to testing the sensors.

At the start of the test, each soil moisture sensor was inserted into a cylinder to obtain the saturated soil moisture value in each of the samples. Then all samples were weighed, by placing them in a metal cup holder (to prevent loss of water from the saturated soil sample), and the weight of the metal cup holder, cheesecloth and PVC cylinder were subtracted. For the next few days the samples were allowed to drain and later on evaporate at the bottom of the cylinder and to evaporate at the top, and the samples were weighted whilst soil moisture was recorded by the sensors. When the soil moisture remained constant the sensors were removed from the samples and the cylinders were placed in a drying oven at 105°C for one day. After cooling, the samples were again weighed and the soil moisture was determined with the sensors. The amount of water present during saturated conditions was determined by subtracting the weight of the sample after drying from the weight of the sample during saturated conditions. Then for each time step the volumetric soil moisture content could be determined by subtracting the weight of the soil sample at that time step from the saturated weight and dividing by the volume of the sample. In Table 9-1, the soil moisture sensor values and the volumetric water content values are displayed. For EC5-1 measurement 9 was used to calculate the total water content and for EC5-2 measurement 7 and for EC5-3 measurement 10 was used.

Calibration lines were determined by the method of least squares with the soil moisture content in mV as input variable (x) and the volumetric soil moisture content as output variable (y), with the following formulas.

$$a = slope = \frac{(n\sum x_i y_i) - (\sum x_i)(\sum y_i)}{(n\sum x_i^2) - (\sum x_i)^2} \qquad \textit{Eq. 3-6}$$

and,

$$b = intercept = \frac{(\sum x_i^3)(\sum y_i) - (\sum x_i)(\sum x_i y_i)}{(n\sum x_i^2) - (\sum x_i)^2} \qquad \textit{Eq. 3-7}$$

With n being the amount of measurements which is 8, 6 and 9 for EC5-1, EC5-2 and EC5-3 respectively. The constructed calibration lines are as follows;

$$y = 8.965x10^{-4}x - 1.161x10^{-2} \qquad \text{EC5-1} \qquad \textit{Eq. 3-8}$$
$$y = 1.293x10^{-3}x - 3.794x10^{-1} \qquad \text{EC5-2} \qquad \textit{Eq. 3-9}$$
$$y = 1.042x10^{-3}x - 2.100x10^{-1} \qquad \text{EC5-3} \qquad \textit{Eq. 3-10}$$

With the raw soil moisture values in mV as input variable x, and the soil moisture content in cm^3/cm^3 as output variable y.

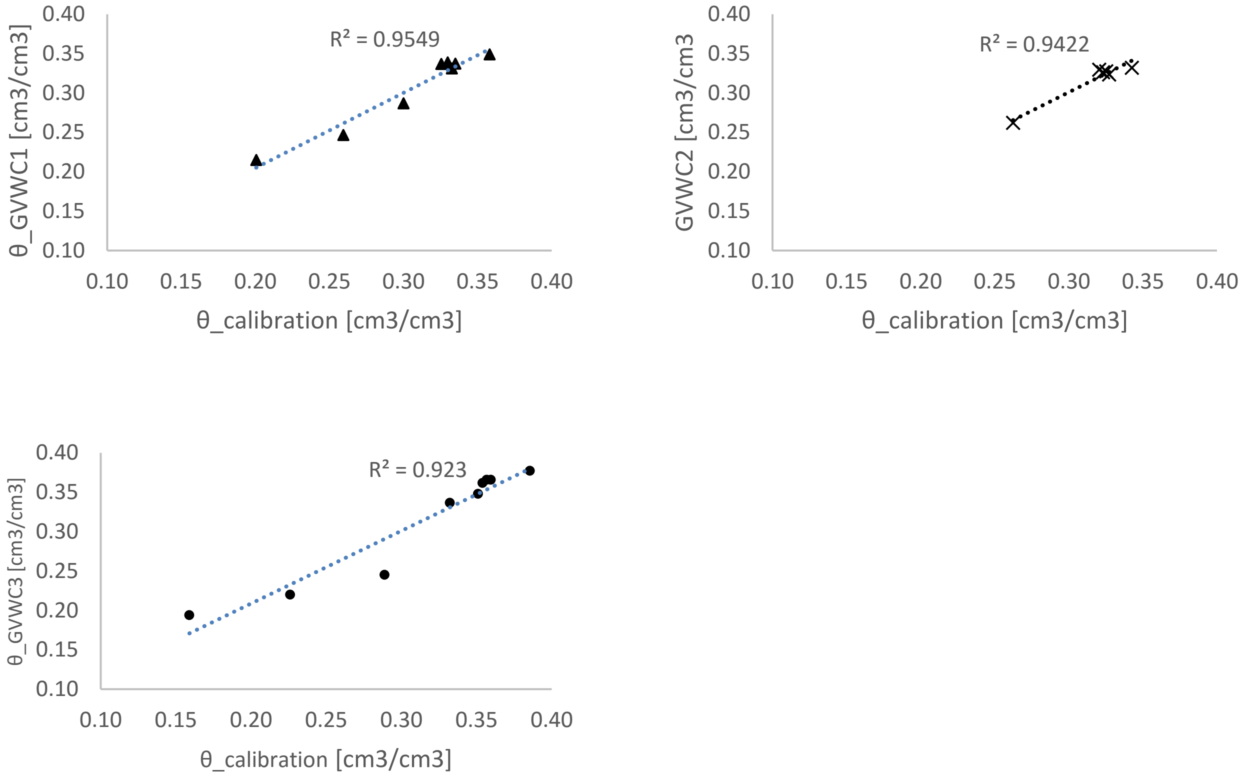

Figure 3-7. The x-axis gives the soil moisture measured by gravimetric measurement and the y-axis gives the soil moisture calculated with the constructed calibration lines. The top left figure is for EC5-1, the top right figure for EC5-2, and the bottom left figure for EC5-3.

R^2 values are relatively low due to of the sensitivity of the sensors and the procedure of testing. The foremost cause is that just before weighing the samples, the soil moisture probe was taken out of the sample (as the electrical cable of the sensor would add extra weight to the sensor and the sensor could not be removed from the data logger). The value of the soil moisture sensor just before taking out the sensor and just after taking out the sensor differed significantly as seen for EC5-1 to EC5-3 in the graph in the appendix (Figure 10-2).

3.3.3 Tensiometers

Six tensiometers were tested by placing the tensiometers vertically (with the membrane downwards) into a 2000 ml beaker glass. The membrane was fully covered in the water (Figure 3-8). As the tensiometers were held vertically the water in the beaker glass was not able to saturate the whole membrane due to gravity. Therefore, the tensiometer reports a negative value even though the porous tip of the tensiometer is fully submerged. It was decided that tensiometer 3 and 4 would not be used in the experiment for two reasons. Firstly, the connection of the sensor to the data logger is not firm enough, which results in NAN (no answer) values. When inserting the sensor with more force to the data logger to re-establish the connection the sensor would still lose contact after some time. Secondly, the vacuum from T4 was often lost, resulting in incorrect matric potential values.

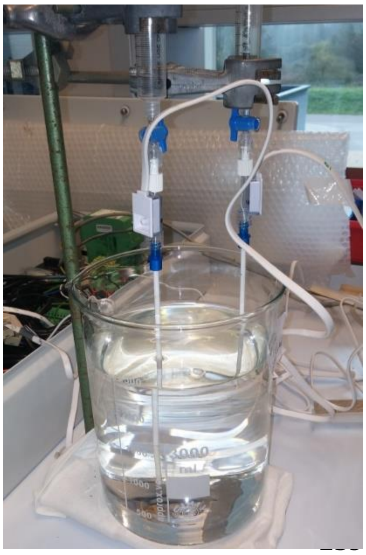

Figure 3-8 Measuring matric potential at different water levels. Here the water level is 7.0 cm above the membrane.

When the tensiometers were tested by placing the tensiometers vertically (with the membrane downwards), the membrane was fully covered in the water and then the water level was raised from 0 to 1, 3, 5 and 7 centimeter. 0 cm of water height is defined as the level at which the only the membrane of the tensiometers is fully covered in the water. The raw data and corrected data values are seen in Table 9-23, 5 and 7 cm of water height.

. The correction has been done by subtracting the matric potential at 0 cm water height from the matric potential measured at 1, 3, 5 and 7 cm of water height.

In Figure 3-9 the matric potential (x-axis) versus the water level is seen (y-axis). The matric potential measured for the different water levels give a good correlation. Slight differences in matric potential may occur due to the tensiometer not being exactly vertical. It can also be that too little or too much water was added into the beaker glass. As the matric potential values from the test are considered to be acceptable, no calibration lines were constructed and raw values from the sensors are used in the results from the experiments.

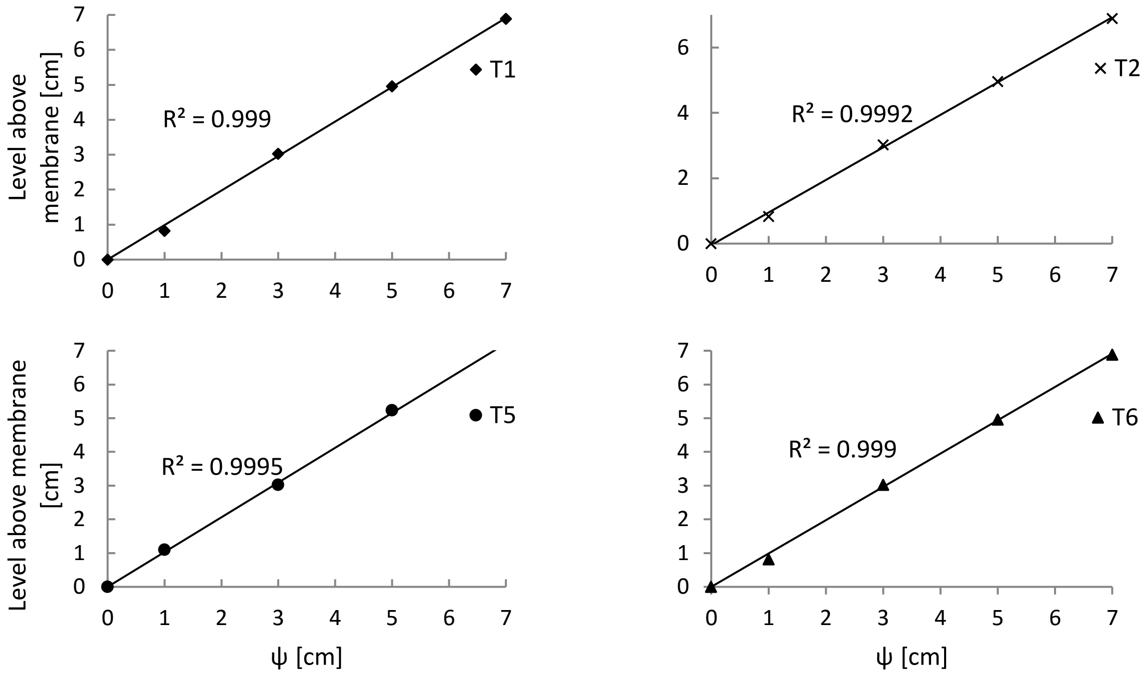

Figure 3-9 Matric potential (x-axis) for T3, T5 and T6 at a water level of 0, 1, 3, 5, and 7 cm above the membrane (y-axis)

3.3.4 Scales

The scales were tested by placing a known weight on the scale and recording the signal given by the sensor in milli-Ampere (Table 3-3). Then the calibration lines were determined by the same procedure (method of least squares) as for the soil moisture sensors For the slope and Eq. 3-7 for the intercept. The recorded signal of the scale as input variable (x, in mA) and the weight as output variable (y, in g) and n = 6. The error in the slope of the calibration lines was is virtually nonexistent seen from the R^2 values in Figure 3-10.

Table 3-3.

Known Weight	Scale A	Scale B	Scale C
[g]	[mA]	[mA]	[mA]
0	4.007	4.008	4.003
2583.86	7.414	7.439	7.509
5177.49	10.832	10.881	11.028
7808.03	14.301	14.373	14.599
10361.59	17.669	17.762	18.067
11427.82	19.078	19.183	19.516

This gives the following calibration lines (with x being mA, and y the weight in g):

$$y = 758.332x - 3037.95$$ Scale A *Eq. 3-11*

$$y = 753.204x - 3018.61$$ Scale B *Eq. 3-12*

$$y = 736.676x - 2947.85$$ Scale C *Eq. 3-13*

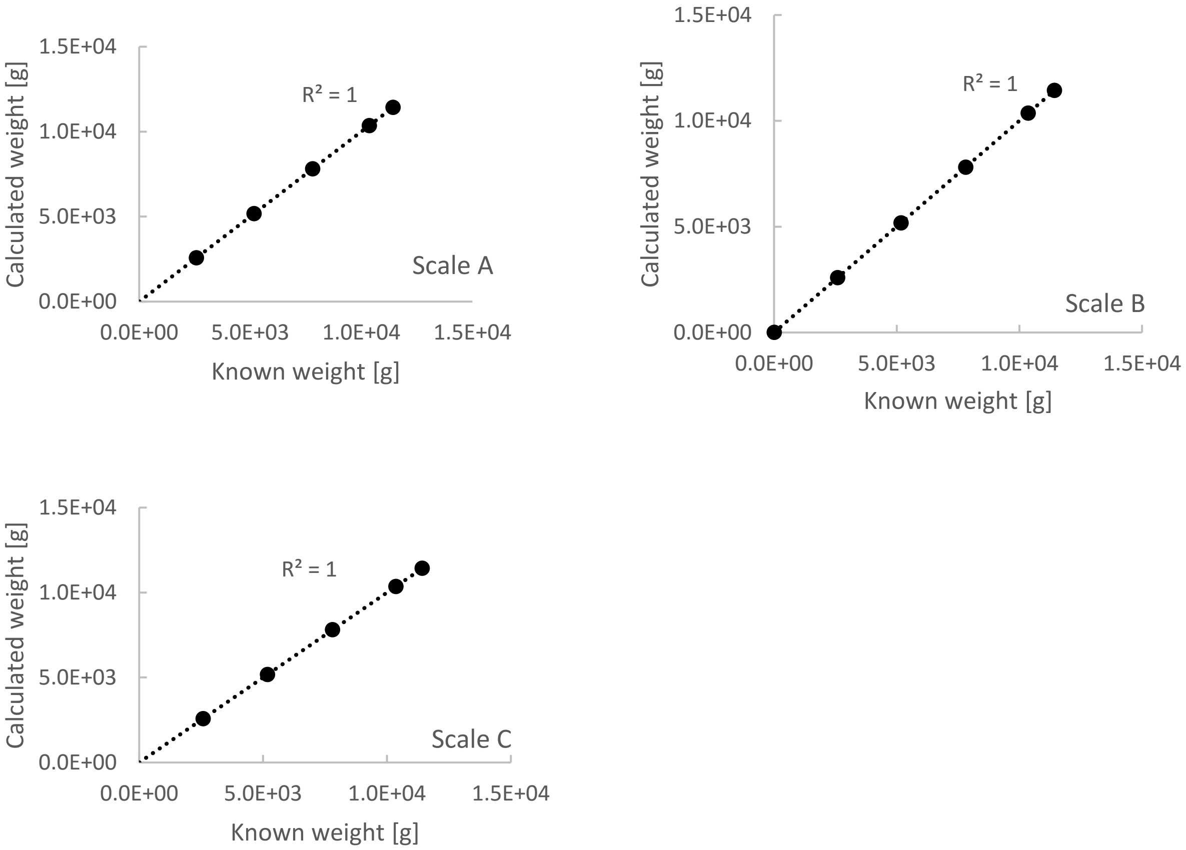

Figure 3-10. Trend lines fitted through known weight data (x-axis) versus calculated weight (y-axis) by the calibration lines.

4 RESULTS EXPERIMENTS

4.1 Soil moisture in experiments: I, II, III, IV and V.

In figure 4.4, the soil moisture profiles are given for experiment I, II and III.

Experiment I, II and III – Soil moisture

In experiment I, the soil moisture content remains constant over time, as was expected as the column is saturated. However the soil moisture values are not the same at all depths (about 0.378, 0.327 and 0.357 cm^3. cm^{-3} at -2.5, -19.0 and -35.0 cm depth) At -19.0 cm depth the soil moisture is about 0.051 $cm.cm^{-3}$ lower at t = 0 h than at -2.5 cm depth.

In experiments II and III (Figure 10-3), at the start, the soil moisture values are lower near the soil surface, due to drainage of the column prior to the start of the experiment. At the start of experiment II it is seen that the soil moisture at -35.0 cm depth in experiment II and III does not change (Table 9-4).The soil moisture values in experiment II, start to rise later at the top (Table 4-1) and attains a constant value later than in experiment III (Table 9-4). This observation is especially noticeable at -2.5 cm depth in the column. Here, the soil moisture is constant after 0.34 hour, in comparison to 0.12 hour in experiment III.

The soil moisture increases only slightly in the long term. After about 20 hours, the soil moisture increased by about 0.5 %, and 0.1 % at -2.5 and -19.0 cm depth in experiment II, in experiment III the soil moisture only rose at the top of the column by 0.4 percent.

In both experiments it is seen that the soil moisture at -19.0 cm depth is lower than at the bottom and top of the column by about 2 to 3 percent. Additionally, in experiment II and III, in which the column was initially drained, the soil moisture remains under the values found in experiment I by 0.1 to 2 %, 20 hours after the start of the experiments.

Table 4-1. Soil moisture values in $cm^{-3}.cm^{-3}$ 0, 0.5 and 1.0 minute after the start of the experiment

	EXP II				**EXP III**		
Time [min]/depth [cm]	**-2.5**	**-19.0**	**-35.0**		**-2.5**	**-19.0**	**-35.0**
0.0	0.253	0.309	0.350		0.250	0.309	0.347
0.5	0.253	0.309	0.350		0.338	0.310	0.347
1.0	0.253	0.309	0.350		0.342	0.313	0.347

Experiment IV and V– Soil moisture

In experiments IV and V (Figure 10-3) the initial value is also lower at the surface than at the bottom of the column due to drainage and at -35.0 cm the soil moisture does not change significantly over the course of the experiment (Table 9-3 and Figure 10-3, appendix).

The soil moisture starts to change much earlier in experiment IV than in experiment V and it also attains a constant value sooner at -19.0 cm depth. At -2.5 cm depth the time at which the soil moisture is constant is difficult to determine due to a slight increase of soil moisture over time. The soil moisture in experiment IV starts to change first at the bottom of the column, due to water infiltrating at the bottom of the column, and in experiment V the water infiltrates at the top of the column.

In experiment IV, the soil moisture at -35.0 cm depth rises by 1.0 % after 1 hour after the start of the experiment. In all other experiment the soil moisture at -35.0 cm depth does not change. At -19.0 cm depth, a constant value is reached very fast (0.02 h). At -2.5 cm a delay is observed, however, the soil moisture rises quickly once the water reaches the sensor.

In experiment V, at -19.0 cm depth, a depression in the soil moisture value of experiment V is observed just before the soil moisture starts to increase. The depression of the soil moisture is about (0.311 -0.306 = 0.005 $cm^3.cm^{-3}$) about 0.5 %. At -2.5 cm depth, it is seen that the soil moisture rises for little until 0.25 h,then it remains constant until 0.079 h and then it rapidly increases until 0.350. After that, a slower increase of soil moisture is seen.

In both experiments (Figure 10-3, appendix) it is also observed that the soil moisture does not attain the same value at all depths. At -19.0 cm depth the value can be up to 4.1 % lower in comparison to the soil moisture value at -2.5 and -35.0 cm depth. After 3 hours the soil moisture has changed maximum by 0.4 %, but at most depths the soil moisture remained constant. Also, the soil moisture values in both experiments, after 3 hours, remain under the soil moisture values found in experiment I, except at -19.0 cm depth (exp. IV and V) and at -35.0 cm (exp. IV).

Table 4-2. Soil moisture values in $cm^{-3}.cm^{-3}$ 0, 0.5 and 1.0 minute after the start of the experiment

	EXP II				**EXP III**		
Time [min]/depth [cm]	**-2.5**	**-19.0**	**-35.0**		**-2.5**	**-19.0**	**-35.0**
0.0	0.245	0.308	0.349		0.248	0.310	0.350
0.5	0.245	0.324	0.353		0.248	0.310	0.350
1.0	0.245	0.331	0.353		0.247	0.311	0.350

4.2 Matric potential in experiments I, II, III, IV, and V.

The matric potential data presented are plotted from the moment the water level in IR1 (Exp. I, II and IV) or the soil column (Exp. III and V) starts to increase. Here, the first hour after the start of the experiments is shown. Data after 3 or 20 hours can be found in the Appendix (Figure 10-7 for Exp. I, Figure 10-8 for Exp. II and III and Figure 10-9 for Exp. IV and V.

Experiment I, II and III – Matric potential.

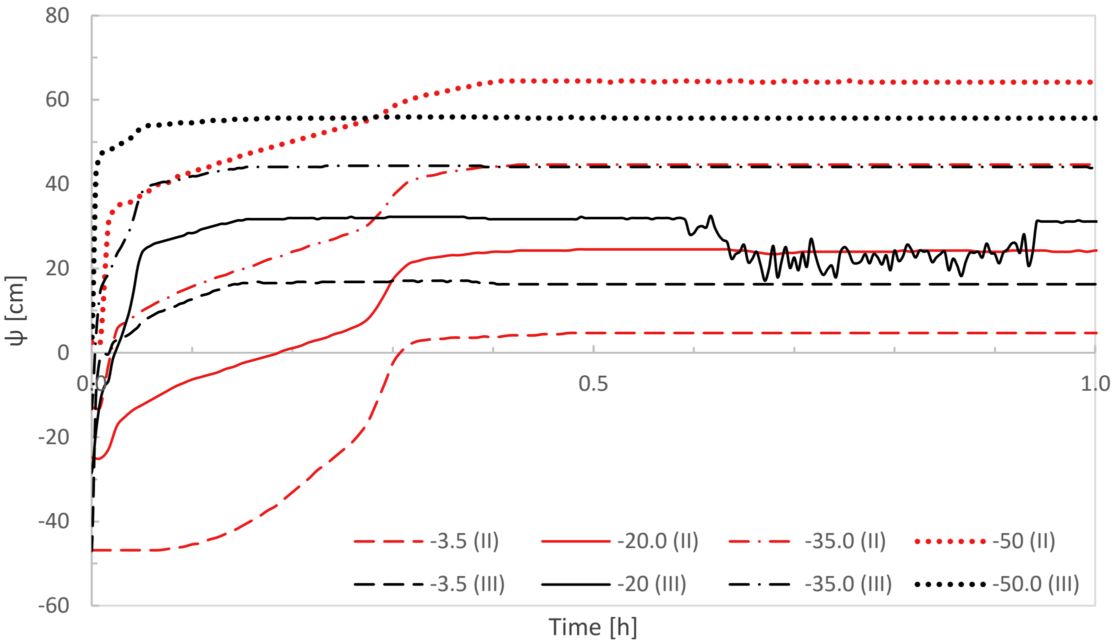

Figure 4-1. Matric potential values over time at -3.5, -20.0, -35.0, and -50.0 cm depth. In experiment II water is infiltrated at the bottom of the column with a total head difference of 12.0 cm, and in experiment III water is infiltrated at the top of the column with a total head difference of 12.5 cm.

In experiment I, the matric potential rises due to the increasing water pressure coming from IR1. When the total head difference was 12.0 cm, the matric potential remained constant throughout time (Figure 10-7). In experiment II and III (Figure 4-2), the total pressure change is larger in comparison to experiment I, as the column was drained prior to the start of the experiment. Therefore, initial values in experiment II and III start out negative at all depths except at -50.0 cm. The matric potential at -50.0 cm starts with a positive value, as the bottom 11 cm of the column is always saturated. In experiment III, the sensor at -20.0 cm depth shows a very wobbly pattern around 0.6. This is caused by insufficient contact of the sensor with the data logger. Pushing the sensor back by manual force fixed the sensor, but it would become lose after some time again.

In experiment I and III, the pressure changes rapidly at all depths just after the start of the experiment, whereas in experiment II a delay is seen in the upper part of the column (Table 4-3). In experiment II, the pressure starts to increase first at -50.0 cm depth, whereas in experiment III the pressure rises at the bottom and the top of the column at the same time. The matric potential values in experiment II attain higher values at the bottom of the column and lower values at the top of the column than in experiment III. This is due to the fact that the pressure at the bottom of the column is around 72.0 cm in experiment II and 60.0 cm in experiment III, while at the top of the column it is 0.5 cm and 13.0 cm, respectively.

Table 4-3. The matric potential in cm at -3.5, -20.0, -35.0 and -50.0 depth at 0, 0.5 and 1 minute after the start of the experiment.

	EXP II					EXP III			
Time [min]/depth [cm]	**-3.5**	**-20.0**	**-35.0**	**-50.0**		**-3.5**	**-20.0**	**-35.0**	**-50.0**
0.0	-46.8	-24.8	-13.0	2.5		-47.1	-28.4	-13.2	2.2
0.5	-46.8	-25.1	-13.0	2.2		-9.9	-18.7	3.9	42.4
1.0	-46.8	-22.9	-2.8	30.9		-0.3	-8.0	17.1	47.7

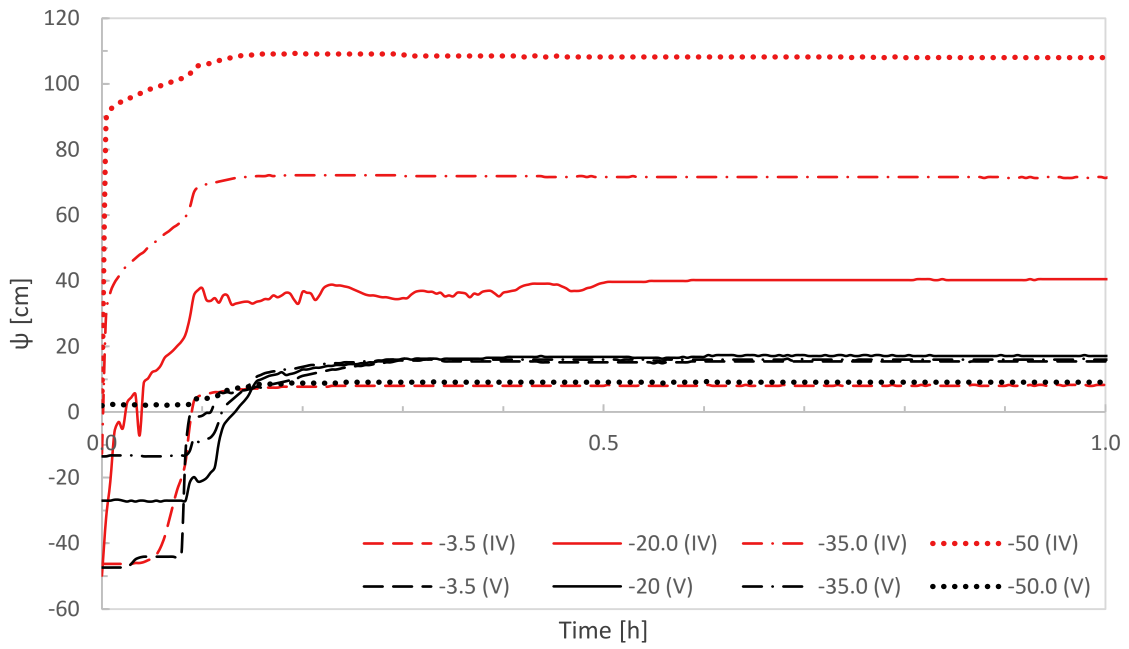

Figure 4-2 Matric potential at -3.5, -20.0, -35.0, and -50.0 cm depth. In experiment IV, the unsaturated outflow was measured (with infiltration the bottom) at a total head difference of 62.9 cm. In experiment V, unsaturated outflow was measured with a total head difference of 61.5 cm, with infiltration occurring at the top of the column.

Experiment IV and V – Matric potential

In experiment IV and V (Figure 4-2), the matric potential starts with the similar values for each depth with 1.1 cm difference at maximum (Table 9-3). Matric potential values in experiment IV starts to rise a lot faster (at 0.0 h, at -50.0 cm depth) than for experiment V (at 0.01 h, -3.5 cm depth) (Table 4-4) and reaches a constant value faster as well (0.23 h for Exp. IV and 0.32 h for Exp. V). Additionally, the final pressure attained in experiment IV is much higher than for experiment V. For example in experiment IV, the pressure is 108.0 cm at -50.0 cm, whereas it is around 9.1 cm in experiment V. The matric potential at -20.0 cm shows a very wobbly pattern after about 0.20 h and should not be interpreted. It is also seen that in experiment V, the matric potential at -3.5 cm first starts to change, then halts for a while (0.025 h), and then it rapidly increases (0.050 h). This is also seen in the sensor at -20.0, -35.0 and -50.0 cm depth, although the effect becomes less prominent deeper in the soil column.

Another observation of experiment V is that the pressure at -20.0 cm depth is first more negative than the pressure at -35.0 cm, but it becomes higher after some time. After about 1.5 hours (Figure 10-9) the matric potential in all sensors suddenly start to decrease in experiment V.

Table 4-4. The matric potential in cm at -3.5, -20.0, -35.0 and -50.0 depth at 0, 0.5 and 1 minute after the start of the experiment.

	EXP IV					**EXP V**			
Time [min]/depth [cm]	**-3.5**	**-20.0**	**-35.0**	**-50.0**		**-3.5**	**-20.0**	**-35.0**	**-50.0**
0.0	-46.3	-49.9	-12.7	3.0		-47.4	-27.0	-13.5	1.9
0.5	-46.3	-21.2	36.4	92.0		-47.4	-27.0	-13.2	2.5
1.0	-46.3	-3.0	41.3	94.2		-47.4	-26.7	-13.2	2.2

4.3 Flux in experiment I, II, III, IV and V.

The fluxes were calculated by subtracting the cumulative weight of each previous time step from the next step. A weight measurement was done every 5 seconds in grams. Thus the flux had to be corrected to present the results to a unit of $cm.h^{-1}$ by dividing by the surface area (1075.2 cm^2), density of water (0.999997 $g.cm^{-3}$), and by dividing by each time step to convert the time steps into hours. For the fluxes a moving average line was fitted through the data by taking the mean of 15 measurements at a time. This was done to reduce the amount of scatter among the data points.

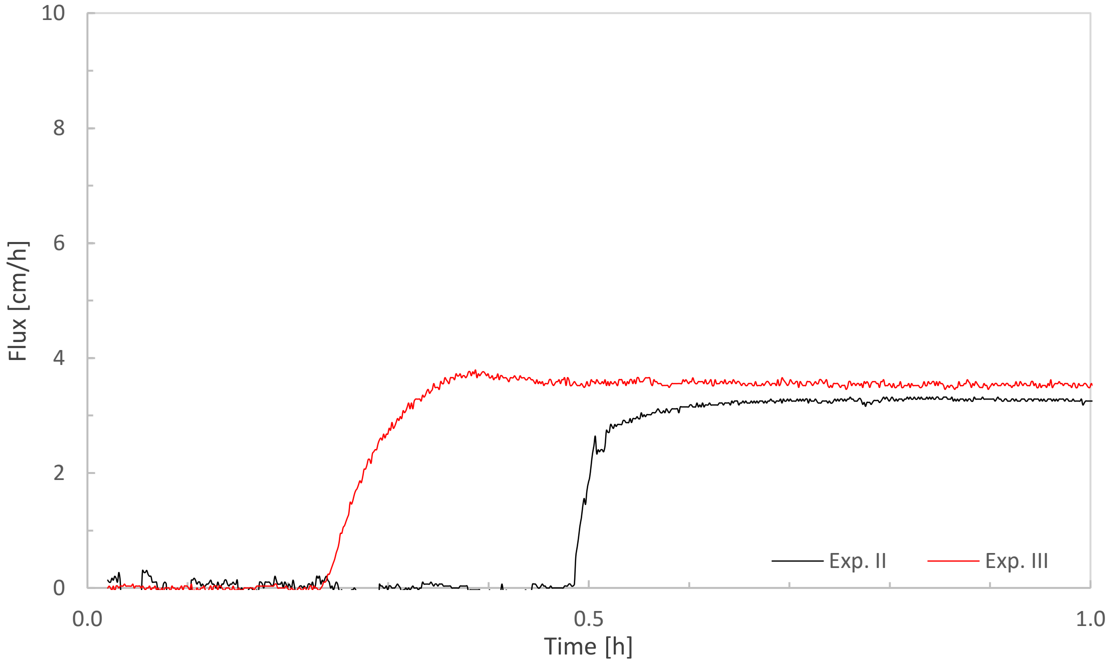

Figure 4-3. In experiment II and III, unsaturated outflow was measured with a total head difference of 12.0 cm, with in experiment II infiltration occurring at the bottom and in experiment III at the top of the column.

4.3.1 Experiment I, II and III – flux.

The flux of experiment I reaches a constant value faster than the flux of experiment II and III, due to the fact that the column is saturated. An average flux has been calculated over several time increments for the flux of experiment I to III (Figure 4-3)

Table 4-5. Average flux values calculated over a time interval of 2 to 3 hours. In the last column the time interval average is not the same for each experiment as the flux was not constant in all experiments.

	Average flux (2 to 3 h) [$cm.h^{-1}$]	Average flux [$cm.h^{-1}$]
Exp. I	3.20	3.09 (45 to 46 h)
Exp. II	3.19	2.98 (17 to 18 h)
Exp. III	3.58	3.52 (7 to 8 h)
Exp. IV	19.47	-
Exp. V	-	18.62 (0.5 to 1 h)

The flux of experiment III starts faster and also stabilizes more quickly than the flux of experiment II. To estimate the value of the constant flux, an average has been calculated between 0.8 and 1.0 hour for both experiments. The average value of the constant flux in experiment II 3.28 cm/h and for experiment III it is 3.53 cm/h.

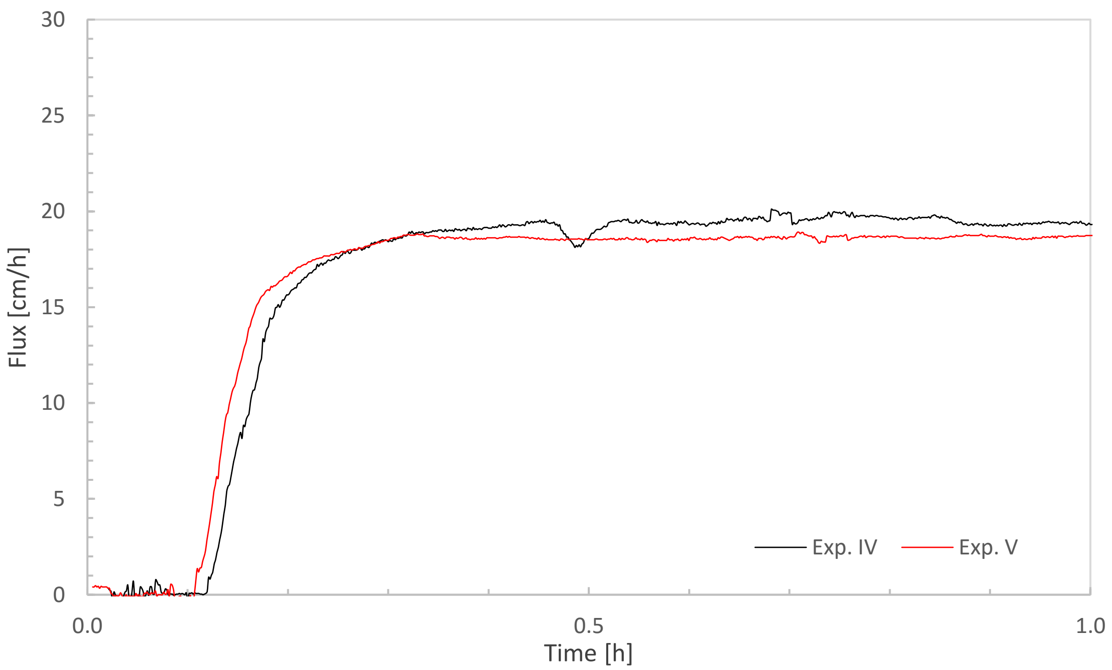

Figure 4-4 Flux in experiment IV and V,

4.3.2 Experiment IV and V - Flux

In Figure 4-3, the fluxes for experiment IV and V are given. Both of the fluxes start at the same time and the flux for experiment IV appears to be slightly larger than for experiment V. At the start of experiment V air bubbles were observed at the top of the column (Figure 4-5). Around, 1.5 hour one can see that the flux in experiment V starts to decrease. The average flux of experiment IV and V has been determined between 1.0 and 1.4 hour after the start of the experiment as the height of the water on top of the column was correct at that point. The constant value of experiment IV is about 19.47 $cm.h^{-1}$ and for experiment V it is 18.62 $cm.h^{-1}$. The flux value of experiment I

Figure 4-5 Experiment V, at the top of the column air bubbles erupted (in the white circle) during the early stages of the experiment, when the ponding layer had not reached its full height yet. The water was supplied by a tap at a height of about 60.0 cm above the soil surface, therefore a grey container was placed, to prevent the falling water from disturbing the soil surface.

4.4 Hydraulic conductivity

For modeling in hydrus-1D the quasi-saturated hydraulic conductivity of experiment I has been determined. Also, the hydraulic conductivities of experiments II to V have been determined to assess the effect of air entrapment on the hydraulic conductivity. In essence, the hydraulic conductivities of all experiments should roughly match, regardless of the pressure difference. It can however be affected by the amount of soil moisture present, which is in turn affected by air entrapment. The hydraulic conductivity has been determined as follows;

$$Q = k_0 * i * A \rightarrow k = \frac{Q}{i * A} = \frac{f}{i} \qquad \textit{Eq. 4-1}$$

In which Q is discharge in $cm^3.h^{-1}$, k is saturated hydraulic conductivity in $cm.h^{-1}$, i is the pressure gradient [-], A is the surface area of the column in cm^2 and f is the flux in $cm.h^{-1}$.

$$i = \frac{\Delta H}{\Delta L} = \frac{(h_1 + z_1) - (h_2 + z_2)}{\Delta L} \qquad \textit{Eq. 4-2}$$

In which;

ΔH	= head difference between the top and bottom of the column	[cm]
h	= matric potential	[cm]
z	= height in the column	[cm]
ΔL	= length of the column	[cm]

The subscript 1 denotes the position at the top of column (0.0 cm depth) and the subscript 2 denotes the position at the bottom of the column (-59.5 cm depth) for experiment I, II and IV. In experiment III and V, subscript 1 denotes the position at the top soil column (0.0 cm depth) and subscript 2 is at the bottom of the soil column (-59.5 cm depth). The pressure gradient and k are determined when the flux has a constant value.

For experiment I:

$$i = \frac{\Delta H}{\Delta L} = \frac{(h_1+z_1)-(h_2+z_2)}{\Delta L} = \frac{(72.0+-59.5)-(0.5+0.0)}{59.5} = 0.202$$

$$k = \frac{f}{i} = \frac{3.20}{0.202} = 15.84\ cm.h^{-1}$$

For experiment II:

$$i = \frac{\Delta H}{\Delta L} = \frac{(72.0\pm 59.5)-(0.5+0.0)}{59.5} = 0.202$$

$$k = \frac{f}{i} = \frac{3.19}{0.202} = 15.79\ cm.h^{-1}$$

For experiment III:

$$i = \frac{\Delta H}{\Delta L} = \frac{(13.0+0.0)-(60.0+-59.5)}{59.5} = 0.210$$

$$k = \frac{f}{i} = \frac{3.58}{0.210} = 17.05\ cm.h^{-1}$$

For experiment IV:

$$i = \frac{\Delta H}{\Delta L} = \frac{(122.9+-59.5)-(0.5+0.0)}{59.5} = 1.057$$

$$k = \frac{f}{i} = \frac{19.47}{1.057} = 18.42\ cm.h^{-1}$$

For experiment V:

$$i = \frac{\Delta H}{\Delta L} = \frac{(13.0+0.0)-(11.0+-59.5)}{59.5} = 1.034$$

$$k = \frac{f}{i} = \frac{18.62}{1.034} = 18.00\ cm.h^{-1}$$

*Table 4-6 Summary of the average outflow flux values, the pressure gradient and the (quasi)-saturated hydraulic conductivities for all the experiments. The correction of the flux value was done for experiments II and IV by using the hydraulic conductivity of experiment II and IV, but the hydraulic gradient of experiment III and V. (For example the corrected flux value of experiment IV is: 18.42 * 1.034 =19.04 cm.h^{-1}.*

	Time interval	i	K	K	Total head difference	Average flux	Corrected average flux
	[h]	[-]	[cm/h]	[m/d]	[cm]	[cm/h]	[cm/h]
Exp. I	2 to 3	0.202	15.84	3.802	12.0	3.20	3.20
Exp. II	2 to 3	0.202	15.79	3.787	12.0	3.19	3.32
Exp. III	2 to 3	0.210	17.05	4.092	12.5	3.58	3.58
Exp. IV	2 to 3	1.057	18.42	4.421	62.9	19.47	19.04
Exp. V	0.5 to 1.0	1.034	18.00	4.320	61.5	18.62	18.62

The flux values need to be corrected for the difference in total head for each experiment. The flux value of experiment II and IV were corrected to the total head difference of experiment III and V, by using the k-value found in experiments II and IV and the hydraulic gradient of experiment III and V.

For experiment II: 15.79*0.210 = 3.32 $cm.h^{-1}$

For experiment IV: 18.42*1.034 = 19.04 $cm.h^{-1}$

Thus, the flux from experiment III is still higher than the flux of the corrected experiment II. The flux in experiment IV is still higher than the flux in experiment V. The ratio between the experiment IV and V is; 0.98. A ratio for experiments II and III is not calculated as it would be higher than 1.

4.5 Hydraulic gradient at the start and end of each experiment

Experiment I, II, and III.

In the initial stage of the column experiment it was proposed to create a ponding layer of 50.0 from 0.0 cm depth in IR1 (thus a pressure of 109.5 cm at the bottom of the column). However, this idea was quickly discarded because of the resulting high gradient (0.832) filled up the scales on the container too fast making measurements at night impossible. Thus, then it was decided to lower the height of the overflow point in IR1 from 50.0 to 12.0 cm (which later turned out to be 12.5 cm) to lower the hydraulic gradient. Then, experiment I (Figure 4-6 b) was conducted successfully, with a final hydraulic gradient of about 0.202. It started with a pressure of 0.0 cm at the top of the column and +60.0 cm at the bottom. The final hydraulic gradient ($i_{f,I}$) is higher due to the ponding layer being 12.5 cm (thus pressure at the bottom of 72.0 cm).

$$i_{i,I} = \frac{(60.0 + -59.5) - (0.0 + 0.0)}{59.5} = 0.008$$

$$i_{f,I} = \frac{(72.0 + -59.5) - (0.5 + 0.0)}{59.5} = 0.202$$

When moving on to the second experiment (Figure 4-6 c), at which the column is drained at the start of the experiment, it causes a swift movement water into the column at the bottom due to the column being drained (resulting in a much higher initial hydraulic gradient;

$$i_{i,II} = \frac{(60.0 + -59.5) - (-48.5 + 0.0)}{59.5} = 0.824$$

At the end of the experiment, (when the column is quasi saturated and the ponding layer is constant), the hydraulic gradient is similar to the final hydraulic gradient of experiment I.

In experiment III (Figure 4-6d), a ponding layer of 13.0 cm was built on top of the soil column. The water height in IR1 was initially set at 0.0 cm (at the soil surface), so that seemingly the total head difference could build up from 0.0 to 12.5 cm. Yet, at the start of the experiment the total head at the bottom of the column is 60.0+-59.5 = 0.5 cm (when V3 is opened) and at the top it is -48.5+0.0= -48.5 cm.

$$i_{i,III} = \frac{(-48.5 + -0.0) - (60 - 59.5)}{59.5} = 0.824$$

Therefore, water will start to flow rapidly from the bottom to the top (just as in experiment II) (Table 4-3, Figure 4-1), until the total head at the top of the column is larger than the total head at the bottom of the column. Due to the rapid pressure increases observed in experiment III and infiltration at the top, the values become constant sooner (0.15 h in comparison to 0.40 h in experiment II).The rapid movement of the water into the soil column in experiment II and III is also confirmed by soil moisture (Figure 10-3)..

One could argue to first keep V3 closed until the water layer on top of the column has reached the overflow point at 13.0 cm (OF1) (although this would not reflect natural conditions). This could work if the water on top of the column does not form fingers and air does not escape. Otherwise, infiltration in experiment III starts earlier than in experiment II.

In the design of the experiment III, the fast inflow of water at the bottom of the column was not anticipated and does not reflect the desirable condition at which the water table remains at a fixed position. The upwards moving water table of experiment III makes comparison to experiment II not possible in terms of the arrival time of the flux. Also, it is unclear how large the effect of the water table movement is on trapping and compressing air between the wetting front and water table. Thus, no conclusion can be drawn from the difference in the flux values of experiment II and III. Therefore, these two experiments will not be modelled or further discussed in this thesis.

Hydraulic gradient at the start and end of experiment IV and V.

In experiment IV(Figure 4-6), the water enters the column very fast as the initial height of the water is at 50.0 cm above the reference point (soil surface). Thus, the initial pressure at the bottom of the column is 110.0 cm. It was set at +50.0 cm height in order to build up the ponding layer difference from 50.0 to 62.9 cm.

$$i_{i,IV} = \frac{(110.0 + \ -59.5) - (-48.5 + 0.0)}{59.5} = 1.660$$

$$i_{f,IV} = \frac{(122.9 + \ -59.5) - (0.5 + 0.0)}{59.5} = 1.057$$

In experiment V, the initial ponding layer is 0.0 cm and builds up to 13.0 cm.In experiment V (Figure 4-6 e), the outflow is at V2 (at -48.5 cm depth), and the water can only flow downwards (as V3 was closed). Here, the water hydraulic gradient at the start of the experiment is;

$$i_{i,V} = \frac{(0.0 + 0.0 - (11 + \ -59.5)}{59.5} = 0.815$$

$$i_{f,V} = \frac{(13.0 + \ 0.0) - (11.0 + -59.5)}{59.5} = 1.034$$

It is seen that the hydraulic gradient at the start of experiment IV is twice as high as the hydraulic gradient at the start of experiment V. This results in a rapid movement of water into the soil column (Table 4-4, Figure 4-2). In order for the conditions to be the same at the start of the experiment the pressure at the bottom of the column in experiment IV should have been 59.5 cm;

$$i_{i,IV} = \frac{(59.5 + \ -59.5) - (-48.5 + 0.0)}{59.5} = 0.815$$

At the end of the experiment, the pressure at the bottom of the column would then have to be 121.5 cm;

$$i_{i,IV} = \frac{(121.5 + \ -59.5) - (0.5 + 0.0)}{59.5} = 1.034$$

During, experiment IV the water level in IR1 would then have to rise by (121.5-59.5 = 62.0 cm). This is unfortunately not comparable to experiment V for two reasons. Firstly, in experiment V the ponding water layer is 13.0 cm, whereas in experiment IV it would be 62.0 cm. Secondly, the ponding water layer in experiment V directly infiltrates into the soil, whereas the buildup of the pressure from 59.5 to 121.5 cm in experiment IV is in IR1 (which would have to be fully filled with water). This means that it is not known how fast the water level in IR1 should be increased, to mimic the buildup of the ponding water layer in experiment V. As the hydraulic gradient at the start of experiment IV is not similar to the hydraulic gradient at the start of experiment V, the results of this pair of experiments cannot be compared.

The error in experiment IV is an experimental design error. There should be a way to achieve the same total head difference at the start of experiment IV as in experiment V, but so far no other solution has been found without making large changes to the experimental set up. Thus, experiment IV will not be modeled and its results will not be further used in the discussion.

It is, however, possible to compare the flux of experiment I by the flux of experiment V (if adjusting for the hydraulic gradient difference). Also, the flux of experiment V can be compared to the flux of scenario V.

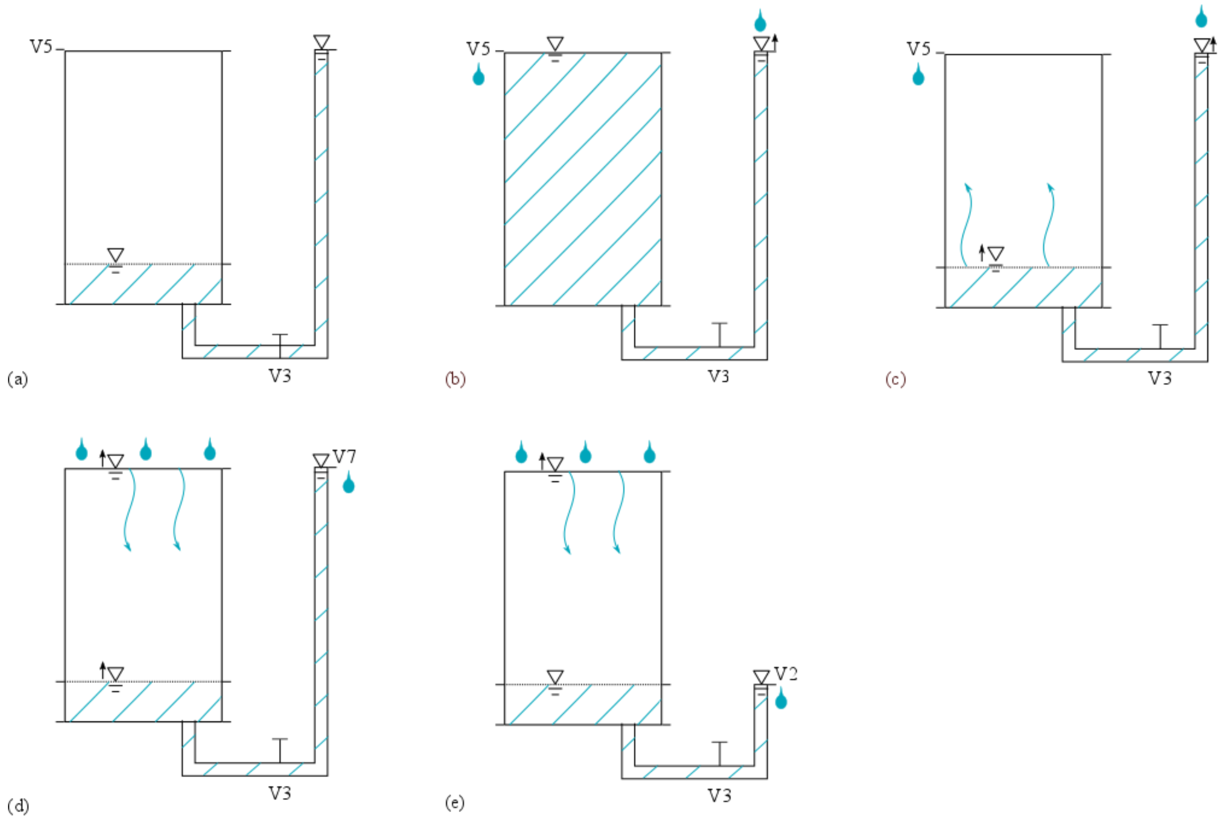

Figure 4-6.(a) Drained start conditions just before opening V3 and the tap for experiments II – V. In (b),(c), (d) and (e) the starting conditions just after opening the tap and V3 are depicted for experiment I, II and IV, III and V, respectively. The starting conditions of experiment II and IV are both in (c), the only difference is that the water level in IR1 at the start of experiment IV is at +50.0 cm, and in experiment II at 0.0 cm.

5 HYDRUS MODELING

The experiments were modeled in Hydrus-1D in order to gain more understanding of the matric potential values, soil moisture and outflow fluxes observed in the experiments. Experiment V will be modeled as scenario V, abbreviated as SCE.V. At first, the column was allowed to drain from saturated conditions for 92.81 hours for SCE.V (similar as in the experiment). Then, the drainage profile was used as the initial matric potential profile the experiment. The input values for the drainage scenario and SCE.V in hydrus-1D can be found in Table 9-5.

In the model a single porosity model is used (van Genuchten-Mualem) (Eq. 5-1).

$$\theta = \theta_r + \frac{\theta_s - \theta_r}{(1 + (\alpha * \psi)^n)^m} \qquad \textit{Eq. 5-1}$$

In which θ is soil moisture, θ_r is the soil moisture at residual soil moisture content (0.057 $cm^3.cm^{-3}$), θ_s is the soil moisture content at saturation (0.372 $cm^3.cm^{-3}$), and ψ is the matric potential. α, m and n are parameters dependent on the shape of the θ(ψ) curve. The parameter m is simplified to m= 1 – 1/n. θ_s, θ_r are known (0.372 and 0.057, respectively). To obtain values for α, m and n the model was fitted to experiment data. The matric potential and soil moisture drainage data are taken from drainage data of experiment II at 92.28 h (Table 5-1). The model was plotted through the data and by altering α and n, the optimal values could be found. The matric potential sensors being used (-3.5, -20.0, and -35.0 cm depth) are not all situated at the same height as the soil moisture sensors (-2.5, -19.0, -35.0 cm depth), though for convenience it is assumed the sensors are at -3.5, -20.0 and -35.0 cm depth. The fitted values for m, n and α are 0.411, 1.700 and 0.036, respectively (Figure 5-1).

Table 5-1. Matric potential and soil moisture data after 92.28 hours of drainage before conducting experiment II.

Depth	ψ	log (-ψ)	θ	
[cm]	[cm]	[cm]	[cm^3/cm^3]	
-3.5	-46.83	1.671	0.253	
-20.0	-24.74	1.394	0.309	
-35.0	-12.95	1.112	0.350	

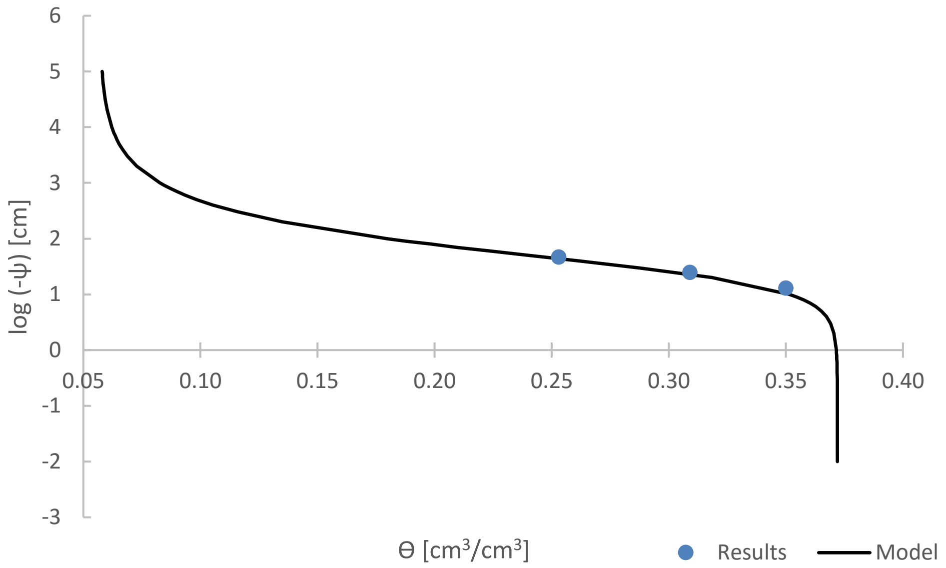

Figure 5-1. Fitting data to hydrus 1D model parameters. α and n were adjusted until the model provided the best fit to the data.

Boundary conditions

In this section, the boundary conditions used in the scenario V and the drainage scenario is explained. In scenario V with a variable pressure head, it must be noted that the pressure head is increased by small increments in a certain time span. There was no data available of the height of the water layer on top of the column in experiment V due to erroneous settings of the sensor. The time span to reach a constant pressure was derived from matric potential data.at -3.5 cm depth.

Scenario drainage – The drainage scenario has a fixed head of 11.0 cm at -59.5 cm depth as a *lower boundary condition*. In the experiments, the outflow point V2 is at -48.5 cm depth, whereby the bottom 11.0 cm of the column remains saturated. The upper boundary condition is a constant flux of 0.0 cm.h^{-1}.

Scenario V – The total head difference between the top and bottom of the column is 12.0 cm when the flux has reached the outflow point. From there the final pressure at the bottom was calculated by using the same formulas as in section 3.2.13.1.1. In scenario V, the *upper boundary condition* is a variable pressure head and the *lower boundary condition* fixed head of 11.0 cm. The pressure at the bottom of the column is 11.0 cm as the bottom 11.0 cm is always saturated. The total head difference is 62.5 cm, from which the pressure at the top of the soil column can be calculated (h_2);

$\Delta H = 62.5$ cm, $z_2 = 0.0$ cm, $h_1 = 11.0$ cm, and $z_1 = -59.5$ cm, thus $h_2 = 62.5 - (11.0 + -59.5) - 0.0 = 14.0$ cm. For scenario V the pressure is built up in 0.32 hours after which the pressure remains constant.

5.1 Initial conditions

5.1.1 Initial conditions

Initial conditions drainage

In the drainage model scenario V, complete saturation was assumed. The soil moisture will be 0.372 cm^3cm^{-3} and the matric potential is +59.5 cm at the bottom of the column and 0.0 cm at the top of the column. The matric potential values in before drainage before experiment V is slightly higher than the matric potential in the drainage scenarios (Table 5-2). This occurs mostly in the lower part of the column (at -35.0 and -50.0 cm depth). Matric potential sensors typically measure over a range of -8,000 to +10,000 cm, therefore, a difference of 2.3 cm is considered accurate

It is seen that the soil moisture values before drainage before experiment V are not at saturation (Table 5-2). The lowest soil moisture found is 4.1% lower than saturation at -19.0 cm depth.

Table 5-2 Matric potential and soil moisture conditions in the soil column before the start of drainage. No values are given for experiment I, as for this experiment the soil was quasi saturated. The saturation time is the time from the start of the previous experiment to the start of the next experiment.. The lowest row denotes the values inserted into hydrus-1D for the drainage scenario.

Start conditions drain	Matric potential				Soil moisture			Saturation time
Experiment / Depth [cm]	-3.5	-20.0	-35.0	-50.0	-2.5	-19.0	-35.0	
	[cm]				[$cm^3.cm^{-3}$]			[h]
V	4.4	22.9	38.6	54.3	0.368	0.331	0.350	55.3
SCE	3.5	20.0	35.0	50.0	0.372	0.372	0.372	-

Initial conditions experiment V versus SCE. V.

The initial conditions of scenario V was compared to the initial conditions of the experiment V. The initial matric potential values of the experiment V (Table 5-3) lie close to the values of SCE.V. It was found that at the top of the column, the offset between the experiment and scenario was slightly higher than in the bottom of the column. At the top (-3.5 cm depth) of the column the matric potential value of Exp.V is 1.5 cm more negative. The more negative matric potential at -3.5 cm depth is not caused by evaporation, as the soil moisture value in the experiment is even lower than the value in the scenario, while the scenario was modelled with evaporation (0.0029 $cm.h^{-1}$). At -20.0 cm depth the matric potential offset is larger, however, this sensor is not reliable enough to take the larger offset into consideration. At -35.0 and -50.0 cm depth the maximum offset is 0.8 and 1.5 cm, respectively. This means that values in the lower part of the column are slightly more positive. Matric potential sensors typically measure over a range of -8,000 to +10,000 cm, therefore, a difference of 2.3 cm is considered accurate. The initial soil moisture values of the experiment and scenario compare reasonably well. In the middle of the column a larger offset is found, with a maximum of 2.1 % in experiment V at -19.0 cm depth.

Table 5-3 Matric potential and soil moisture conditions in the soil column before the start of drainage. No values are given for experiment I, as for this experiment the soil was quasi saturated. The saturation time is the time from the start of the previous experiment to the start of the next experiment. If the quasi saturation time is high then the soil moisture is expected to be relatively high as well. The lowest row denotes the values inserted into hydrus-1D for the drainage scenario

Start conditions experiments	Matric potential				Soil moisture			Drainage time
Experiment / Depth [cm]	-3.5	-20.0	-35.0	-50.0	-2.5	-19.0	-35.0	
	[cm]				[cm^3.cm^{-3}]			[h]
V	-47.4	-27	-13.5	1.9	0.248	0.310	0.350	92.81
SCE	-45.1	-28.5	-13.5	1.5	0.248	0.289	0.340	-

5.2 Scenario V

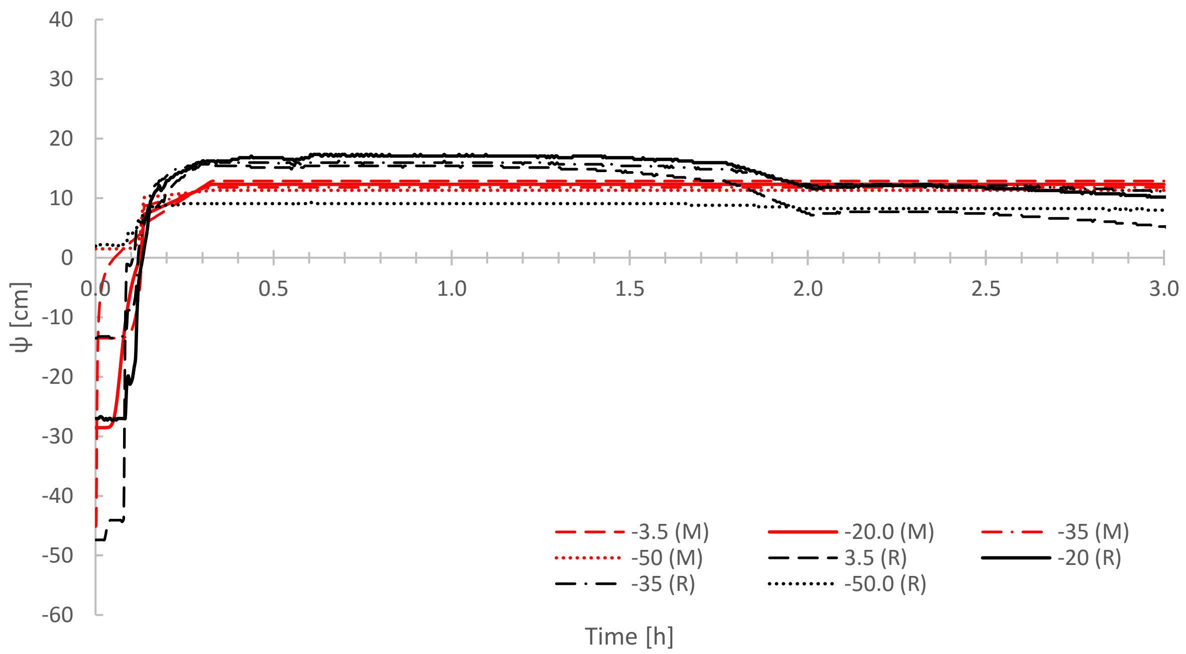

Figure 5-2 Matric potential in scenario V, water is infiltrated at the top of the column, with a total head difference of 62.5 cm between the bottom of the column (H_2 = -49.5 cm) and the top of the column (H_1 = 13.0).

The matric potential profiles of the scenario match quite well in terms of timing. The values are slightly lower for the model and the in the experiment one can see that the matric potential values in the middle of the column (-20.0 and -35.0 cm depth) are higher than at -3.5 and -50.0 cm depth. While in the scenario one can see that the matric potential becomes higher with depth. The matric potential in SCE.II does not diminish after 1.5 hour. Also, at the start one can see that the matric potential immediately starts to increase at -3.5 cm depth, after that -20.0, -35.0 and -50.0 cm depth follow. In the experiment a delay is observed of the matric potential change at -3.5 cm.

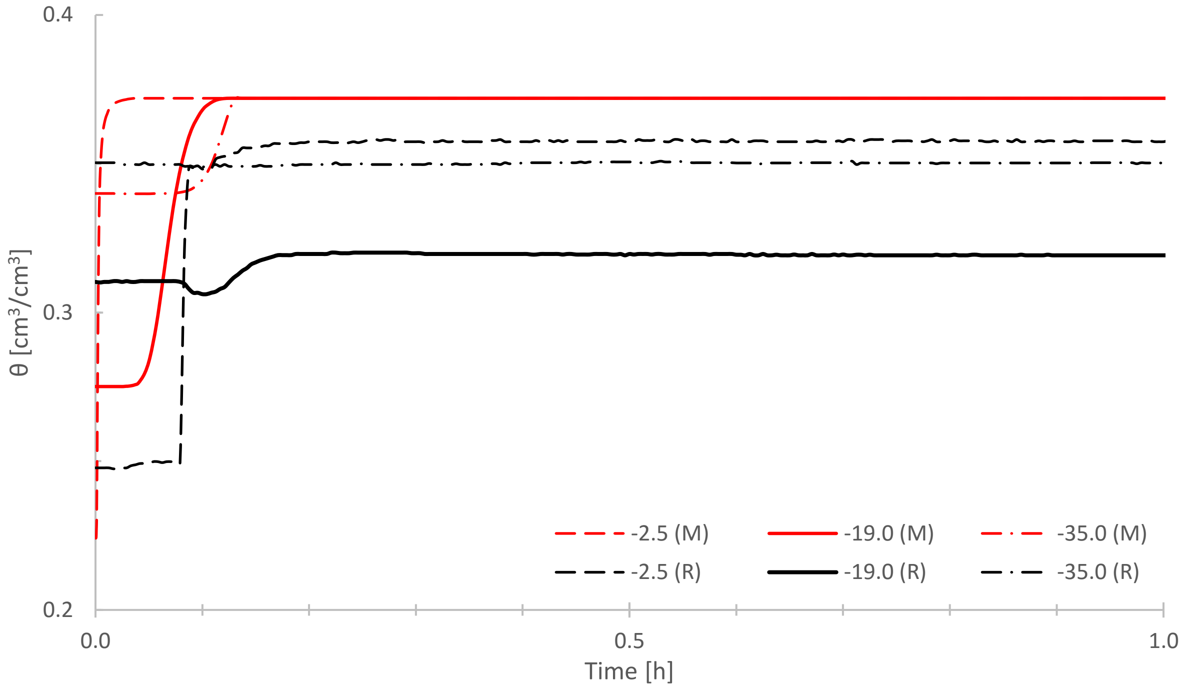

Figure 5-3 Soil moisture experiment V. In scenario V, water is infiltrated at the top of the column and exists at the bottom of the column, with a total head difference of 62.5 cm

In the soil moisture graph (Figure 5-3), the soil moisture at -2.5 cm in the scenario starts to increase immediately, whereas in the experiment the soil moisture has a delay of around 0.079 h (4.7 min). Though, the delay does not seem to affect the time at which the soil moisture becomes starts to change at -19.0 cm depth. In the soil moisture values it is seen that in experiment V a steady value is reached at around 0.18 h and in the scenario at 0.11 h. This may the earlier constant value of the value in the scenario.

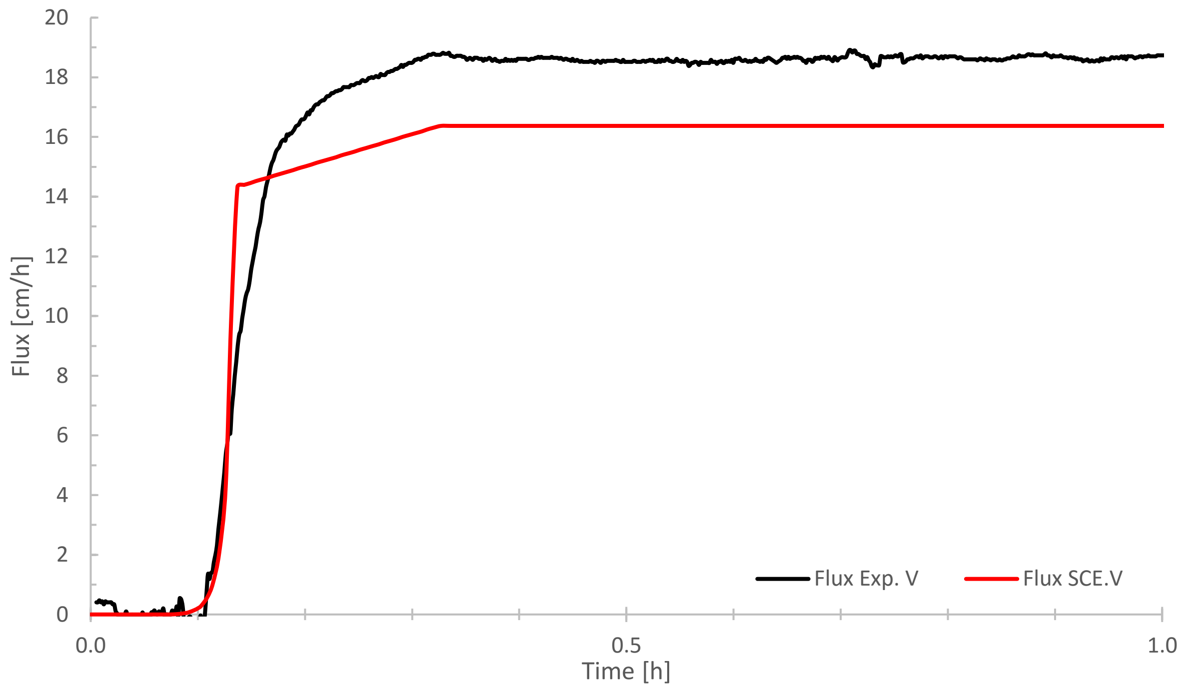

Figure 5-4 In scenario V, water is infiltrated at the top of the column with a total head difference of 62.5 cm between the bottom of the column and the top of the soil column. The model results are given as F M (red line) and the model results are given as F R (black line).

In Scenario V, the arrival time of the flux is the same as in the experiment. The magnitude of the flux is however, not the same. In the experiment the magnitude of the flux is about 19.47 $cm.h^{-1}$, whereas in the model it is 16.40 $cm.h^{-1}$. This leads up to a difference of 0.74 $m.d^{-1}$.

One can see that in the model and experiment the matric potential has not reached its constant value yet, when the flux starts. The matric potential achieves a constant value around 0.33 hour for both the model and the experiment, while the flux starts around 0.100 hour.

6 Discussion

6.1 Patterns in the matric potential, soil moisture and flux values of experiment V.

In experiment V, the sensor at -3.5 cm depth responds directly at the start of the experiment. The column is being sealed by the water infiltrating at the top and the water table residing in the soil column at -48.5 cm depth. The same behavior has also been observed in the simulations of the experiments in Hydrus-1D, which means that water infiltrates from the top downwards.

In experiment V it was observed that the matric potential at -20.0 cm depth is first lower than the matric potential a -35.0 cm depth, but becomes higher after some time. This phenomena is caused by the wetting front moving down the soil column. At first when the wetting front has not passed -20.0 and -35.0 cm depth yet, the matric potential at -20.0 cm will be more negative than at -35.0 cm depth due to drainage of the column. At the moment the wetting front passes the sensor at -20.0 cm depth the matric potential will increase at that point while at -35.0 cm depth the matric potential is still mostly defined by the drainage before the start of the experiment. The shape of the matric potential over depth flips around when the column is quasi saturated (from 0.25 to 51.65). This is due to the fact that the pressure at the outflow point is about 0.0 cm and at the top of the column the matric potential is 13.0 cm due to the ponding layer. The matric potential lines in this experiment lie close together due to the small matric potential difference inside the column. At V2 atmospheric conditions apply and at the top of the column a pressure of 13.0 cm is applied. Therefore, we see a non-linear behavior in the soil column with the highest matric potential in the middle of the column.

After 1.5 hours the matric potential in all sensors and flux value reduced (even before the peak), while this did not happen in SCE.V. The reduction in the matric potential after 1.5 hours is due to the fact that the tap was not supplying sufficient water to keep the ponding layer constant. Unfortunately, this statement cannot be supported by Keller data for experiment V (to get the ponding height directly) as the apparatus was installed with the wrong settings.

Also the flux values in both experiments from about 1.67 to 1.95 h are increased due to emptying of the outflow containers. During this procedure the tap remained on while the outflow valve (V2 for experiment V) was shortly closed to prevent outflow from being discharged outside of the outflow container A, B and C during emptying. During this time water built up at the ponding layer, while the overflow point was not large enough to discharge the excess water. This increases the flux for a short period of time. The increase in pressure on top of the column was also seen in the graph of the matric potential, but it has been filtered out.

When comparing SCE.V and Exp.V flux development, it was seen that the flux of the experiment arrives at the same time as the in the modelling scenario. It was expected that the flux of the experiment would take longer to arrive at the outflow point V2 due to air being trapped. Additionally, it was expected that the flux in the experiment would arrive later than SCE V as hydrus-1D does not take compression of air into account. In hydrus-1D the water will infiltrate as a sharp wetting front without preferential flow paths (if the sand is homogeneous). Also, the magnitude of the flux in experiment V is higher than for SCE.V. The flux in experiment V is probably bigger than the flux in the scenario due to formation of preferential flow paths induced by entrapped air. Several factors indicate the formation of preferential flow paths and presence of entrapped air;

- At the start of experiment V, it was observed in the matric potential data and the soil moisture data that for some time infiltration is halted (0.025 h). Then at 0.079 h (after 4.74 min) it shoots up. At this moment air must have erupted from the soil surface as seen in.
- A depression in the soil moisture was observed at 0.079 at -20.0 cm depth in the column. This depression is only 0.5% and lasts until 0.125 h, after which the value is 0.310 again. This shows that preferential flow is occurring as at that moment the matric potential is increasing rapidly in all sensors of the column. The soil moisture sensor may be in an area at which no preferential flow path was formed until after 0.125 hour.
- The flux starts before soil moisture has reached a constant level at -2.5, -19.0 and -35.0 cm depth. For example, the soil moisture at -2.5, and -19.0 cm depth is constant at 0.17 and 0.19 h, while the flux starts around 0.10 hour. The matric potential inside the column is also not constant yet, but this is due to the fact that the ponding layer on top of the soil had not reached 13.0 cm yet.
- The hydraulic conductivity calculated for experiment V is higher than for experiment I. In experiment I the hydraulic conductivity is 15.84 $cm.h^{-1}$, and in experiment V it is 18.42 $cm.h^{-1}$. This is a difference of 2.58 $cm.h^{-1}$(equal to 61.9 $cm.d^{-1}$).

The preferential flow paths formed in the column could be due to wall flow, but the fact that matric potential increases earlier than the soil moisture provides evidence that preferential flow also occurs within the sand column itself. It can however, not be assessed if there is wall flow, and if yes, how much does it contribute to the flux.

6.2 The effect of compressed air

In literature the effect of air compression was assessed by dividing the unconfined flux by the confined flux. Although, it was attempted to divide the flux of experiment V by the flux of experiment V, however, since the confined flux (V) is affected by preferential flow (which makes the flux arrive earlier, and possibly also attain a higher flux) this value cannot be taken as very reliable. The ratio is then; 18.62/19.04 = 0.98 (when corrected for extra total head difference). The ratio between experiment IV and V shows that the effect of air entrapped air on the flux of experiment V is not great on the long term. Thus, it can be concluded that for this soil that air is not easily trapped between the wetting front, even though, the wetting front was withheld from advancing from 1.5 to 4.7 minutes after the start of experiment V.

There can be there various factors contributing to a limited effect of air compression;

- *Air wall flow* - During experiment V, in which water was infiltrated at the top of the column, air bubbles emerged at the top of the column. Most of the bubbles escaped along the column wall and some in the middle of the ponding water layer. The eruption of air bubbles tells that the pressure of the air between the wetting front and the water table exceeded the air entry pressure and the pressure of the overlying water layer or that there is air flow along the column wall. The escape of air bubbles allows more space for water to flow through the soil, by which the outflow rate will increase, and thus a smaller effect of air compression. The air can escape via the column walls due to improper packing of the soil by which space between the sand grains and column wall exists. The air space between the soil in the column and the column wall can serve as a preferential pathway for water or air (Sentenac et al. 2001; Corwin 2000). The preferential pathway will cause instabilities near the wetting front, which can cause more preferential flow pathways for either air or water. However, there is evidence that preferential sidewall flow occurs even when no space or gap exists due to an increase in the permeability of the soil in contact with the sidewall (Schoen et al. 1999). Sentenac et al. (2001) observed that the flow velocity at a column wall can be between 1.11 and 1.45 times the flow velocity in the column centre.

  They also observed that wall flow increases with larger soil particle sizes and that it is more exaggerated at small hydraulic gradients. A grainsize of 0.3 to 0.6 mm resulted in less effect of wall flow than for a grainsize of 0.6 to 1.2 mm. The grainsize in this experiment ranges from 0.09 to 0.52 mm, with the median around 0.23 mm. Thus part of the soil in the column may let air or water flow preferentially along the column walls.

  The authors (Collis-George and Bond, 1981) evaluated the pressure of trapped air behind the wetting front. After the infiltration experiment with an initially dry soil, the soil column was drained and infiltration started again. This time, no sharp increase of air pressure in encapsulated air near the wetting front was found. It is thought that during drainage of the column, the sand in the column shrinks slightly, leaving a small space between the column wall and the sand and also around the sensors in the column. This creates continuous air spaces, in which it does not matter where the position of the wetting front is. This might have happened in the column experiment conducted in this study as well, as the soil column was repeatedly drained.
- Wall flow can also make the outflow flux higher by flowing along the column wall. One can detect wall flow when the soil moisture and matric potential in the column do not start to change at the same moment. In experiment V it is indeed seen that the matric potential rises before the soil moisture starts to rise. In scenario V, the matric potential changes first, and shortly after the soil moisture starts to change. As hydrus-1D does not incorporate wall flow, it cannot be stated that if soil moisture or matric potential starts to change earlier than the matric potential or soil moisture, there is wall flow per se.

- *The grainsize* of the soil column has an influence on the capacity to retain the air between the wetting front and water table. In a study by Franzini (1966) it was suggested that soil mediums with a geometric mean larger than 0.3 mm are not effective at retaining air, since the air entry value is easily exceeded. The grainsize of the sand used in this column has a range of 0.1 mm to 0.5 mm, with the mean at 0.23 mm. Thus about 50 % of the soil particles have a grainsize between 0.23 and 0.50 mm. The plausibility of wall flow or a too large grainsize is supported by the appearance of air bubbles near the column wall and in the middle of the column within minutes after the start of the experiment V.

- *The capillary rise* of the soil was also not estimated correctly, due to the fact that the initial parameters inserted in hydrus-1D were not specifically for this soil, and therefore the capillary rise was estimated to be less high than it is in reality. The capillary rise is extending to a greater height than initially expected. The soil moisture at -35.0 cm in the column only changed very minimally upon drainage of the column, and at the top of the column (-3.5 cm depth) the difference between saturated and drained conditions was only about 10% (Table 9-4). This problem could be solved by selecting either a larger grainsize, draining the column for a longer time or a longer column. When opting to fill the column with a larger grainsize, this would not reflect the grainsize found in the areas with infiltration ponds in the dunes. Also, as discussed before soils with an effective grainsize more than 0.3 mm are less effective in retaining air. On the contrary a longer column would result in less effect of the capillary rise and allow for low soil moisture values at the top of the column.

6.3 Effect of entrapped air

The presence of entrapped air is difficult to assess as there are only three sensors measuring the soil moisture in the soil column. Additionally, the calibration lines of the soil moisture sensors were proven not to be very reliable. In most of the data however, it was observed that the soil moisture was not at its saturation value as found in the gravimetric soil moisture (0.372 $cm^3.cm^{-3}$) obtained from the in situ core (section 3.3.1). The highest values found in experiment I were 0.383, 0.328 and 0.358 $cm^{-3}.cm^{-3}$, while at that point the column was saturated for a long time by letting water flow through the column. At the end of experiment V, the soil moisture values are 3.0, 0.5 and 0.9 % below the maximum values found in experiment I. Thus, it can be said that on average the amount of entrapped air is not very high. In the middle of the column lower soil moisture values were repeatedly reported

It is noticeable that in the middle of the column the soil moisture is 4.8 % lower than the gravimetrically determined soil moisture (0.372 $cm^3.cm^{-3}$) at saturation at the end of experiment V. It is not clear why the values are lower in the middle of the column. The sand was homogeneously mixed before it was put into the soil column. There may be a local depression in the porosity due to differences in the force applied when tamping down the sand in the column.

6.4 Improving the column experiment

- For further research using this column set up, it is suggested to increase the roughness of the column wall with sand paper or gluing sand to it (Sentenac et al. 2001). Due to the roughness of the inner wall of the column, sand grains may pack better and prevent side wall flow. One can also install annular rings on the interior surface of the column prior to the addition of soil (Corwin, 2000).
- Another improvement would be increasing the column length. A column length of 59.5 cm has proven to be too small as the capillary rise extended beyond -35.0 cm depth whereas the water table was situated at -48.5 cm depth. The increase in column length will make it further dehydration possible.
- In experiment III, V3 could be opened when the pressure on top of the column is constant and thereby no water would infiltrate from IR1 as the pressure coming from the ponding layer would be larger. There is however, no easy way to fix the difference in hydraulic gradient at the start of experiment IV. However, if one is not interested in comparing the arrival time of the flux with infiltration from above (Exp V) one could set the pressure at 59.5 cm at the bottom of the column and then increase the water level until the same total head difference is achieved as in experiment V.

7 CONCLUSION

- The effect of compressed air has been seen as a short lived effect in experiment V. There, the air is retained in the first 4.7 minutes after which the air erupts through the surface of the soil column. The ratio between experiment IV and V is 0.98, thus the effect of confined to unconfined infiltration in experiment set IV-V is limited. Literature based values range from very small values to 0.65, though the soils and grainsizes in the literature are very different from the soil used in this experiment. The ratios are most likely high due to the fact that air was able to escape at the surface of the column and preferential flow paths increased the flux of experiment V. The escape of air is attributed to air wall flow and water wall flow, and the column length being too small by which the capillary rise is too high (in comparison to the column length) to effectively retain the air between the wetting front and the water table as the air entry pressure is low.
- The effect of entrapped air is minimal when compared to the maximum soil moisture values attained in experiment I, ranging from 0.5 to 3 percent.
- To make the column experiment more successful;
  1. The column length should be increased;
  2. The column wall should be roughened to prevent air and water flow along the column wall;
  3. And lastly, for experiment III, V3 should be opened at the moment when the s

8 REFERENCES

Adrian, D.D., and Franzini, J.B., (1966). Impedance to infiltration by pressure build-up ahead of the wetting front. J. Geophys. Res. No 71: 5857 – 5862.

Collis-George, N., Bond, W.J., (1981). Ponded infiltration into simple soil systems: 2. Pore air pressures ahead of and behind the wetting front. Soil Science 131, No 5: 263 – 270.

Corwin, D.L., (1999). Evaluation of a simple lysimeter-design modification to minimize sidewall flow. Journal of Contaminant Hydrology, No 42: 35-49.

Domenico, P.A. and F.W. Schwartz, 1990. Physical and Chemical Hydrogeology, John Wiley & Sons, New York, 824 p.

Grismer, M.E., (1994). Effect of air compression and counter flow on infiltration into soils. J. of irrigation and drainage engineering 120: 775 – 795.

Faybishenko, B.A., (1995). Hydraulic behavior of quasi-saturated soils in the presence of entrapped air: Laboratory experiments. Water. Resour. Res. 31: 2421 – 2435.

Jing, Z., Gong, H., Ross, M. A., Li, X., Zhou, D., (2011). Numerical modeling of shallow water table behavior with Lisse effect. Chin. Geogra. Sci. 21: 249 – 256.

Kools, S.A.E. et al (2008). Verkenning geneesmiddelen en toxiciteit effluent RWZI's. STOWA rapport. 2008-06.

Konyai, S., Sriboonlue, V., Trelo-Ges, V., (2009). The effect of air entry values on hysteresis of water retention curve in saline soil. American Journal of Environmental Sciences, 5: 341-345.

Mavis, M.T., Tsui, T.P., (1939). Percolation and capillary movements of water through sand prisms. University of Iowa, studies in Engineering, bulletin 18.

Peck, A.J., (1964). Moisture profile development and air compression during water uptake by bounded porous bodies: 2. Horizontal columns. Soil Sci. 99: 327 - 334

Peck, A.J., (1964). Moisture profile development and air compression during water uptake by bounded porous bodies: 3. Vertical columns. Soil Sci. 100: 44 – 51

Or, D., Lehmann, P., Moebius, F., Hoogland, F., (2012). Multi-scale interface in unsaturated soil (figure 3). Retrieved from: http://www.step6.ites.ethz.ch/researches/index/42

Sentenac, P., Lynch, R.J., Bolton, M.D., 2001. Measurement of side-wall leakage in soil columns using fibre-optics sensing. International Journal of Physical Modeling in Geotechnics, 4: 35-41.

Siemens, G.A., Peters, S.B., and Take, W.A., (2013). Comparison of confined and unconfined infiltration in transparent porous media. Water. Resour. Res. 49: 851 – 863.

Vachaud, G., Vauclin, M., Khanji, D., Wakil, M., (1973). Effects of air pressure on water flow in an unsaturated stratified vertical column of sand. Water. Resour. Res. 9: 160 – 173.

Vachaud, G., Gaudet, J.P., Kuraz, V., (1974). Air and water flow during ponded infiltration in a vertical bounded soil column of soil. J. of Hydrology. 22: 89 – 108.

Wakil, M., (1972). Role de phase gezeuse dans l'inifiltration et le drainage d'une colone de sol stratifi. PhD thesis, Univ. of Grenoble, Grenoble France.

Wang, Z.W., Feyen, J., van Genuchten, M.T., and Nielsen, D.R., (1998). Air entrapment effects on infiltration rate and flow instability. Water. Resour. Res. 34: 213 – 222.

Wentworth, J.K., (1922). A scale of grade and class terms for clastic sediments. J. of Geol. 30: 377-392.

Wilson, L.G., and Luthin, J.N. (1963). Effect of air flow ahead of the wetting front on infiltration. Soil Sci. 86: 117 - 125.

9 APPENDIX TABLES

Table 9-1 Calibration measurements of the weight and soil moisture of 3 soil samples to calibrate EC5 soil moisture probes. In the t column (second column) the time is given at which the measurement is taken after the sample was removed from saturated conditions (t = 0.0 h).

Soil sample 1 (EC5-1)						Soil sample 3 (EC5-3)			
Measurement	t	EC5-1	Weight sample	Water content	VWC	EC5-3	Weight sample	Water content	VWC
[#]	[h]	[mV]	[g]	[g]	[$cm^3.cm^{-3}$]	[mV]	[g]	[g]	[$cm^3.cm^{-3}$]
1	0.0	571	927.1	180	0.390	597	921.8	193.8	0.420
2	1.1	556	915.5	168	0.365	584.7	908.7	180.7	0.392
3	2.2	549	914.3	167	0.363	584.7	907.3	179.3	0.389
4	4.1	558	912.9	166	0.360	580.3	905.9	177.9	0.386
5	7.1	556	910.7	164	0.355	565.4	904.5	176.5	0.383
6	30.5	493	897.9	151	0.327	552.8	895.0	167.0	0.362
7	71.6	443	877.5	130	0.283	453.7	873.2	145.2	0.315
8	144.5	403	847.9	101	0.219	426.5	841.6	113.6	0.246
9	-	-	747.1	0	0.000	398	801.3	73.3	0.159
10	-	-	-	-	-	-	728.0	0.0	0.000

Soil sample 2 (EC5-2)					
Measurement	t	EC5-2	Weight soil	Water content	VWC
[#]	[h]	[mV]	[g]	[g]	[$cm^3.cm^{-3}$]
1	0.0	574	891.3	166.9	0.362
2	0.5	560	883.7	159.3	0.346
3	1.1	566	882.8	158.4	0.347
4	2.7	564	881.7	157.3	0.341
5	5.2	570	880.4	156.0	0.338
6	74.2	458	851.8	127.4	0.276
7	-	315	724.4	0.0	0.000

Table 9-2. Vertical test of the tensiometers. The corrected values in column 4 and 5 give a reasonable value to the actual water level above the membrane.

Water level above membrane	Raw ψ		Corrected ψ	
[cm]	[cm]		[cm]	
	T1	**T2**	**T1**	**T2**
0	-16.53	-15.71	0.00	0.00
1	-15.71	-14.88	0.82	0.83
3	-13.50	-12.68	3.03	3.03
5	-11.57	-10.75	4.96	4.96
7	-9.64	-8.82	6.89	6.89
	T6	**T5**	**T6**	**T5**
0	-16.53	-16.81	0.00	0.00
1	-15.71	-15.71	0.82	1.10
3	-13.50	-13.78	3.03	3.03
5	-11.57	-11.57	4.96	5.24
7	-9.64	-9.64	6.89	7.17

Table 9-3. t_{start} gives the time at which the matric potential starts to change at a particular depth, and $t_{constant}$ gives the time at which the matric potential is constant. $\psi_{t=0h}$ gives the initial matric potential, $\psi_{t=constant}$ the matric potential when it is constant, $\psi_{t=1h}$, $\psi_{t=3h}$, and $\psi_{t=20h}$ give the matric potential value after 1, 3 and 20 hours, respectively.

Matric potential							
	Depth	t_{start}	$t_{constant}$	$\psi_{t=0h}$	$\psi_{t\_constant}$	$\psi_{t=1h}$	$\psi_{t=20h}$
	[cm]	[h]	[cm]	[cm]	[h]	[cm]	[cm]
Exp. II	-3.5	0.07	0.48	-46.8	4.7	4.7	4.7
	-20.0	0.02	0.48	-24.8	24.5	24.2	17.4
	-35.0	0.02	0.43	-13.0	44.6	44.6	44.1
	-50.0	0.02	0.41	2.5	64.5	64.2	63.7
Exp. III	-3.5	0.00	0.15	-46.8	16.5	16.3	16.3
	-20.0	0.00	0.15	-28.4	31.7	31.1	31.7
	-35.0	0.00	0.15	-13.2	44.1	44.1	44.1
	-50.0	0.00	0.14	2.2	55.6	55.6	55.9
Exp. IV	Depth	t_{start}	$t_{constant}$	$\psi_{t=0}$	$\psi_{t\_constant}$	$\psi_{t=1h}$	$\psi_{t=3h}$
	[cm]	[h]	[cm]	[cm]	[h]	[cm]	[cm]
	-3.5	0.03	0.23	-46.3	8.0	8.3	7.7
	-20.0	0.00	-	-	-	40.2	39.1
	-35.0	0.00	0.18	-12.7	72.2	71.3	70.5
	-50.0	0.00	0.15	3.0	109.1	108.0	107.4
Exp. V	-3.5	0.01	0.32	-47.4	16.0	15.4	5.2
	-20.0	0.08	0.32	-27.0	16.3	17.1	10.2
	-35.0	0.07	0.32	-13.5	17.0	16.0	11.3
	-50.0	0.08	0.32	1.9	9.1	9.1	8.0

Table 9-4. t_{start} gives the time at which the soil moisture starts to change at a particular depth, and $t_{constant}$ gives the time at which the soil moisture is constant. $\theta_{t=0h}$ gives the initial soil moisture, $\theta_{tconstant}$ the soil moisture when it is constant, $\theta_{t=1h}$, $\theta_{t=3h}$ and $\theta_{t=20h}$ give the soil moisture value after 1, 3 and 20 hours, respectively.

Soil moisture							
	Depth	t_{start}	$t_{constant}$	$\theta_{t=0h}$	$\theta t_{constant}$	$\psi_{t=1h}$	$\psi_{t=20h}$
	[cm]	[h]	[h]	[$cm^3.cm^{-3}$]	[$cm^3.cm^{-3}$]	[$cm^3.cm^{-3}$]	[$cm^3.cm^{-3}$]
Exp. II	-2.5	0.08	0.34	0.253	0.359	0.359	0.364
	-19.0	0.02	0.10	0.309	0.328	0.328	0.329
	-35.0	-	-	0.350	0.350	0.350	0.349
Exp. III	-2.5	0.00	0.12	0.250	0.355	0.354	0.358
	-19.0	0.01	0.10	0.309	0.326	0.327	0.326
	-35.0	-	-	0.347	0.347	0.348	0.347
	Depth	t_{start}	$t_{constant}$	$\theta_{t=0}$	$\theta_{tconstant}$	t=1h	$\psi_{t=3h}$
	[cm]	[h]	[h]	[$cm^3.cm^{-3}$]	[$cm^3.cm^{-3}$]	[$cm^3.cm^{-3}$]	[$cm^3.cm^{-3}$]
Exp. IV	-2.5	0.03	0.17	0.245	0.363	0.363	0.362
	-19.0	0.00	0.02	0.308	0.332	0.322	0.333
	-35.0	0.00	0.04	0.349	0.356	0.360	0.359
Exp. V	-2.5	0.02	0.17	0.248	0.357	0.357	0.356
	-19.0	0.03	0.19	0.310	0.320	0.319	0.323
	-35.0	-	-	0.350	0.350	0.350	0.349

Table 9-5.Matric potential values at the start of scenario V.

Node [#]	Depth [cm]	ψ [cm]		Node [#]	Depth [cm]	ψ [cm]		Node [#]	Depth [cm]	ψ [cm]
1	0.0	-48.7		41	-20.0	-28.5		81	-40.0	-8.5
2	-0.5	-48.2		42	-20.5	-28.0		82	-40.5	-8.0
3	-1.0	-47.7		43	-21.0	-27.5		83	-41.0	-7.5
4	-1.5	-47.2		44	-21.5	-27.0		84	-41.5	-7.0
5	-2.0	-46.7		45	-22.0	-26.5		85	-42.0	-6.5
6	-2.5	-46.1		46	-22.5	-26.0		86	-42.5	-6.0
7	-3.0	-45.6		47	-23.0	-25.5		87	-43.0	-5.5
8	-3.5	-45.1		48	-23.5	-25.0		88	-43.5	-5.0
9	-4.0	-44.6		49	-24.0	-24.5		89	-44.0	-4.5
10	-4.5	-44.1		50	-24.5	-24.0		90	-44.5	-4.0
11	-5.0	-43.6		51	-25.0	-23.5		91	-45.0	-3.5
12	-5.5	-43.1		52	-25.5	-23.0		92	-45.5	-3.0
13	-6.0	-42.6		53	-26.0	-22.5		93	-46.0	-2.5
14	-6.5	-42.1		54	-26.5	-22.0		94	-46.5	-2.0
15	-7.0	-41.6		55	-27.0	-21.5		95	-47.0	-1.5
16	-7.5	-41.1		56	-27.5	-21.0		96	-47.5	-1.0
17	-8.0	-40.6		57	-28.0	-20.5		97	-48.0	-0.5
18	-8.5	-40.1		58	-28.5	-20.0		98	-48.5	0.0
19	-9.0	-39.6		59	-29.0	-19.5		99	-49.0	0.5
20	-9.5	-39.1		60	-29.5	-19.0		100	-49.5	1.0
21	-10.0	-38.6		61	-30.0	-18.5		101	-50.0	1.5
22	-10.5	-38.1		62	-30.5	-18.0		102	-50.5	2.0
23	-11.0	-37.6		63	-31.0	-17.5		103	-51.0	2.5
24	-11.5	-37.1		64	-31.5	-17.0		104	-51.5	3.0
25	-12.0	-36.6		65	-32.0	-16.5		105	-52.0	3.5
26	-12.5	-36.1		66	-32.5	-16.0		106	-52.5	4.0
27	-13.0	-35.6		67	-33.0	-15.5		107	-53.0	4.5
28	-13.5	-35.1		68	-33.5	-15.0		108	-53.5	5.0
29	-14.0	-34.6		69	-34.0	-14.5		109	-54.0	5.5
30	-14.5	-34.1		70	-34.5	-14.0		110	-54.5	6.0
31	-15.0	-33.6		71	-35.0	-13.5		111	-55.0	6.5
32	-15.5	-33.1		72	-35.5	-13.0		112	-55.5	7.0
33	-16.0	-32.6		73	-36.0	-12.5		113	-56.0	7.5
34	-16.5	-32.1		74	-36.5	-12.0		114	-56.5	8.0
35	-17.0	-31.5		75	-37.0	-11.5		115	-57.0	8.5
36	-17.5	-31.0		76	-37.5	-11.0		116	-57.5	9.0
37	-18.0	-30.5		77	-38.0	-10.5		117	-58.0	9.5
38	-18.5	-30.0		78	-38.5	-10.0		118	-58.5	10.0
39	-19.0	-29.5		79	-39.0	-9.5		119	-59.0	10.5
40	-19.5	-29.0		80	-39.5	-9.0		120	-59.5	11.0

Table 9-6 Input values model for the drainage and scenarios I to V.

Parameter	Unit	Scenario	
Name scenario	-	Drainage	SCE.V
Main processes	-	Water flow	
Number of soil materials	-	1	
Depth of soil profile	cm	59.5	
Initial time	hours	0.0	
Final time	hours	92.81(V)	3.0
Initial time step	hours	0.02	1.67E-05
Minimum time step	hours	0.002	1.67E-06
Maximum time step	hours	0.4	1.67E-02
Time variable boundary conditions	[#]	-	58
Number of print times	-	4	6
Print times	hour	0.005; 0.5; 20.0; 91.35	0.01; 0.02; 0.03; 0.1; 0.5; 3.0
Iteration criteria	-	All default values	
Soil hydraulic model	-	Single porosity (van Genuchten-Mualem)	
Hysteresis	-	No	
Saturated soil water content (Qs)	-	0.372	
Residual soil moisture content (Qr)	-	0.057	
Alpha	1/cm	0.036	
n	-	1.70	
Saturated hydraulic conductivity (Ks)	cm/h	15.84	
Turtuosity (I)	-	0.21	
Upper boundary condition	cm/h	Constant flux (=0.0)	Variable pressure head
Lower boundary condition	cm	Constant head (11.0 cm)	Constant head (11.0 cm)
Time variable boundary conditions	-	None	Yes, 58.
Initial conditions	cm	at z = 0.0, h = 0.0 and at z = -60.0 → h = 60.0 (as soil is saturated)	h profile imported from drainage model, profile at t = 92.81(V) hours
Nodes	#	120	
Observation nodes	cm	0.0; -2.5; -3.5; -19.0 -20.0; -35.0, -50.0; -59.5	

843

Table 9-7. t_{start} gives the time at which the matric potential starts to change at a particular depth, and $t_{constant}$ gives the time at which the matric potential is constant. $\psi_{t=0h}$ gives the initial matric potential, $\psi_{t=constant}$ the matric potential when it is constant, $\psi_{t=1h}$, $\psi_{t=3h}$, and $\psi_{t=20h}$ give the matric potential value after 1, 3 and 20 hours, respectively.

	Depth	t_{start}	$t_{constant}$	$\psi_{t=0h}$	$\psi_{t\_constant}$
	[cm]	[h]	[cm]	[cm]	[h]
SCE V	0.0	0.00	0.33	-48.7	13.0
	-3.5	0.00	0.34	-45.1	12.9
	-20.0	0.03	0.33	-28.5	12.3
	-35.0	0.06	0.33	-13.5	11.8
	-50.0	0.07	0.33	1.5	11.3
	-59.5	-	-	11.0	11.0

Table 9-8. t_{start} gives the time at which the soil moisture starts to change at a particular depth, and $t_{constant}$ gives the time at which the soil moisture is constant. $\theta_{t=0h}$ gives the initial soil moisture, $\theta_{tconstant}$ the soil moisture when it is constant

	Depth	t_{start}	$t_{constant}$	$\theta_{t=0h}$	$\theta t_{constant}$
	[cm]	[h]	[h]	[$cm^3.cm^{-3}$]	[$cm^3.cm^{-3}$]
SCE. II	0.0	0.12	0.32	0.243	0.372
	-2.5	0.13	0.38	0.248	0.372
	-19.0	0.03	0.18	0.289	0.372
	-35.0	0.002	0.01	0.340	0.372
SCE. III	0.0	0.00	0.0	0.243	0.372
	-2.5	0.01	0.03	0.248	0.372
	-19.0	0.03	0.07	0.289	0.372
	-35.0	0.002	0.01	0.340	0.372
SCE. IV	Depth	t_{start}	$t_{constant}$	$\theta_{t=0}$	$\theta_{tconstant}$
	[cm]	[h]	[h]	[$cm^3.cm^{-3}$]	[$cm^3.cm^{-3}$]
	0.0	0.07	0.11	0.243	0.372
	-2.5	0.06	0.11	0.248	0.372
	-19.0	0.02	0.04	0.289	0.372
	-35.0	0.001	0.004	0.340	0.372
SCE. V	0.0	-	-	0.243	0.372
	-2.5	0.001	0.03	0.225	0.372
	-19.0	0.04	0.11	0.275	0.372
	-35.0	0.08	0.13	0.340	0.372

Table 9-9. The arrival time of the flux (t_{start}), the time at which the flux is constant ($t_{constant}$) and the flux value $q_{constant}$ at $t_{constant}$.

	t_{start}	$t_{constant}$	$q_{constant}$
	[h]	[h]	[cm/h]
SCE. II	0.32	0.42	3.18
SCE. III	0.07	0.18	3.33
SCE. IV	0.10	0.12	1.68
SCE. V	0.11	0.33	1.64

10 APPENDIX FIGURES

Sympatec GmbH
System-Partikel-Technik

WINDOX

Particle Size Analysis

Sympatec HELOS (H1408) RODOS: Bodemzand 10/12/15 / 14:23:28

feeder:	N.N. unknown		Measuring conditions:	LMA-A2		
pressure:	3.00	bar	measuring range:	R5: 0.5/4.5...875µm		
vacuum:	10.00	mbar	measuring duration:	10.01		s
feed rate:	50.00	%	cycle time:	1000		ms
funnel gap:	5.00	mm	start when:	0.50%	at	C.Opt
revolution:	60.00	%	reference measurement:	00:00:21 ,	0.00 %	
			evaluation:	LD (V 3.4 Rel.1)		
			parameter 4	:		

Operator : JP
Identifier : 314888/5 KWR C-15 2716
Comments:

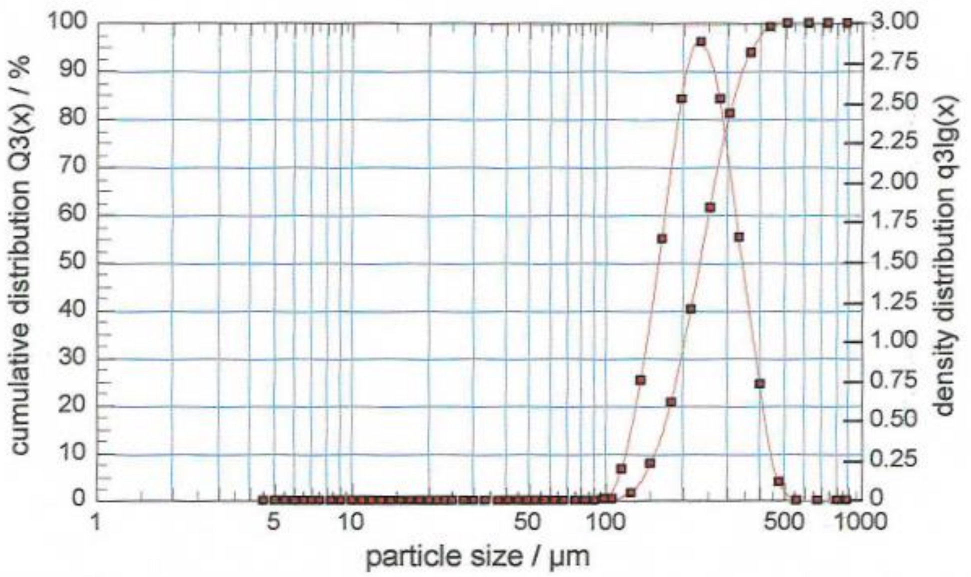

Volume Size Distribution

x0/µm	Q3/%	x0/µm	Q3/%	x0/µm	Q3/%	x0/µm	Q3/%
4.50	0.00	18.50	0.00	75.00	0.00	305.00	80.71
5.50	0.00	21.50	0.00	90.00	0.00	365.00	93.62
6.50	0.00	25.00	0.00	105.00	0.03	435.00	99.16
7.50	0.00	30.00	0.00	125.00	1.48	515.00	100.00
9.00	0.00	37.50	0.00	150.00	7.36	615.00	100.00
11.00	0.00	45.00	0.00	180.00	20.35	735.00	100.00
13.00	0.00	52.50	0.00	215.00	39.78	875.00	100.00
15.50	0.00	62.50	0.00	255.00	61.09		

x10 =	156.10 µm	x50 =	234.18 µm	x90 =	348.18 µm
x60 =	252.95 µm	x84 =	320.29 µm	x99 =	432.94 µm
VMD =	244 µm	Sv =	0.0269 m2/cm3	c_opt =	0.53 %

Figure 10-1 Grain size analysis of the sand used in the column experiment

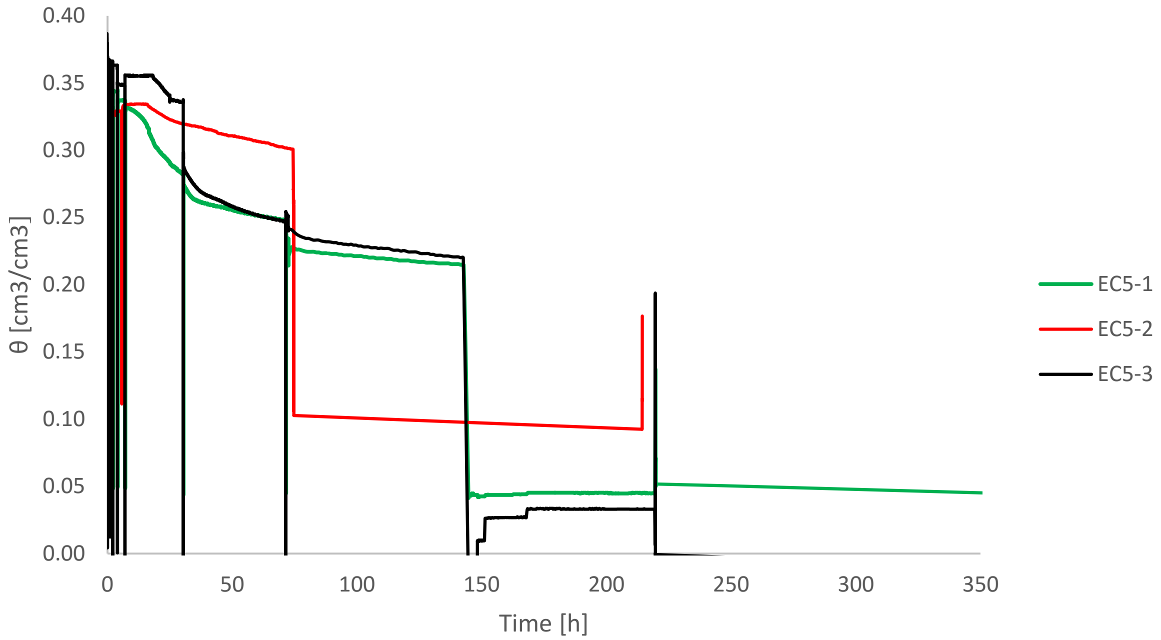

Figure 10-2 Soil moisture over time during drying out of a soil sample in order to obtain a calibration line for EC5-1. The jumps in soil moisture content mark the moments at which the probe was removed from the sample to be able to weigh the soil sample.

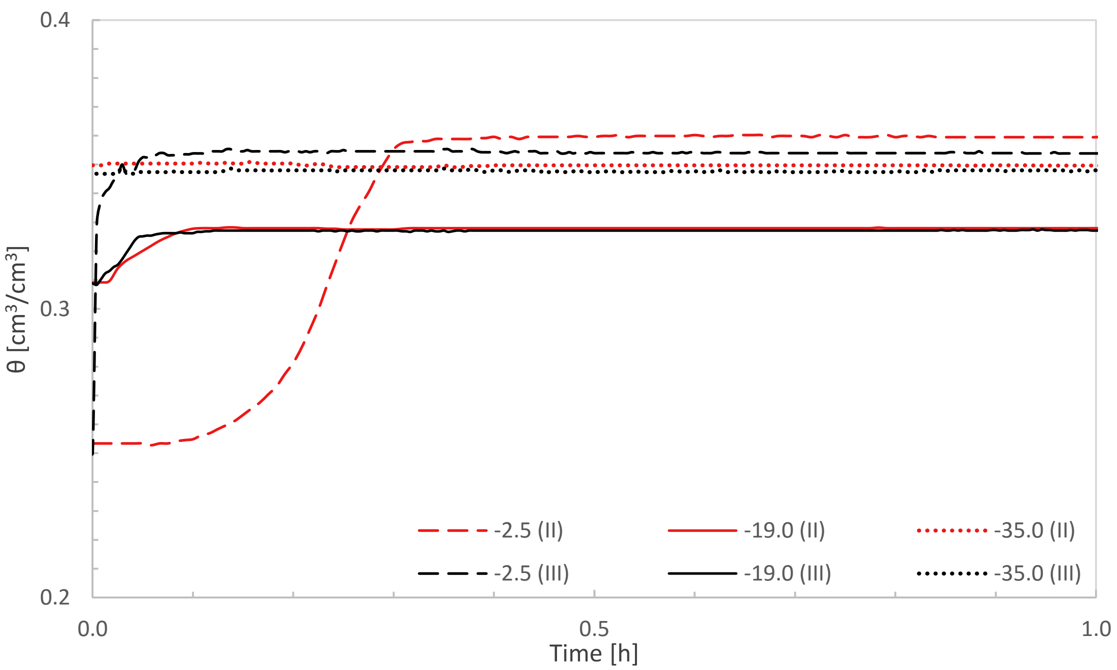

Figure 10-3. Soil moisture values at -2.5, -19.0 and -35.0 cm depth in experiment II and III.

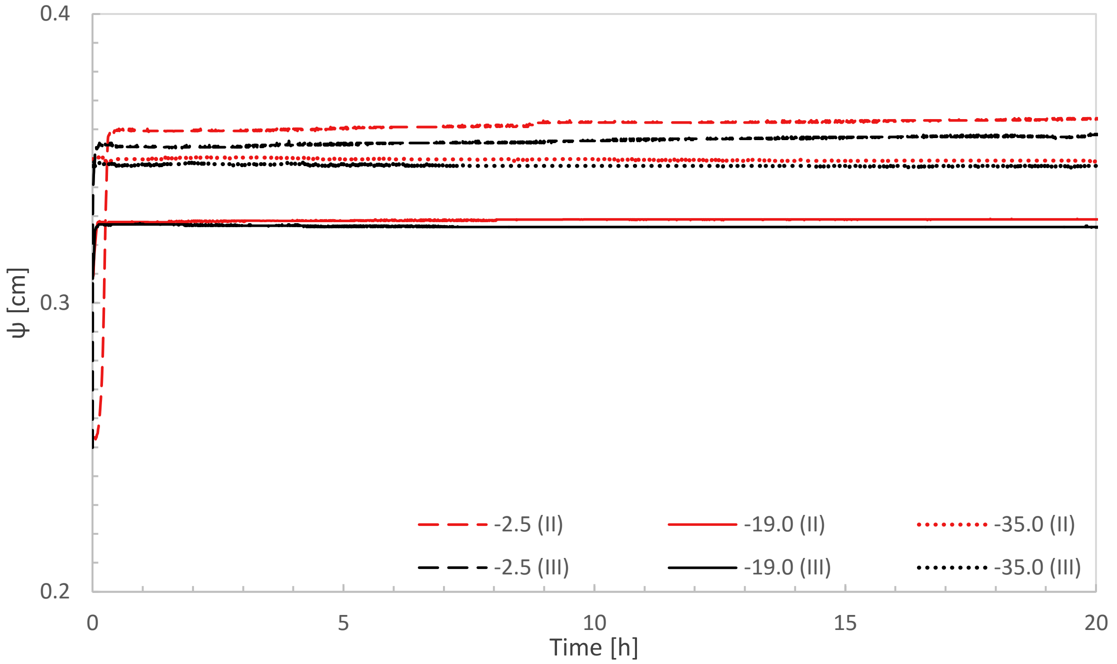

Figure 10-4. Long term soil moisture values at -2.5, -19.0 and -35.0 cm depth in experiment II and III.

853

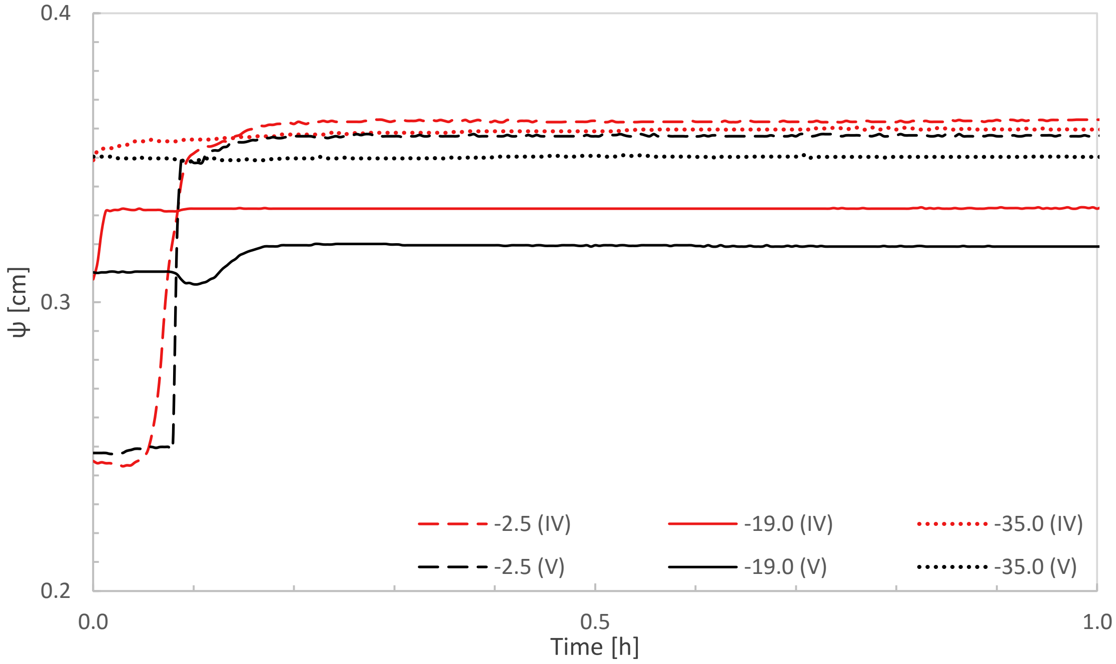

Figure 10-5. Short term soil moisture values in experiment IV and V at -2.5, -19.0 and -35.0 cm depth

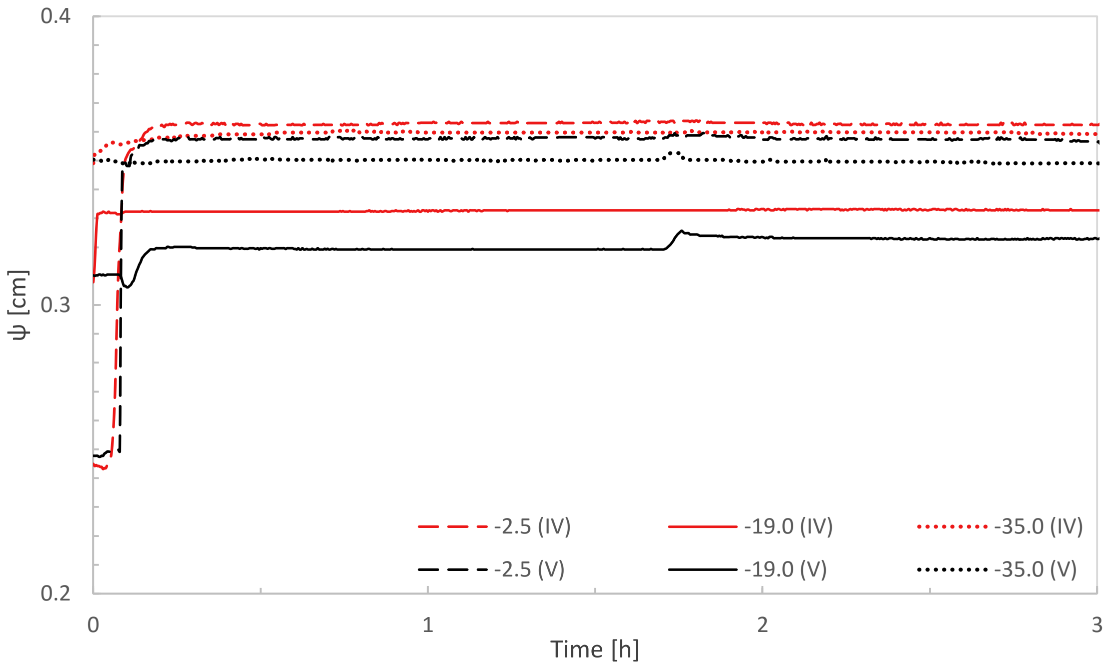

Figure 10-6. Long term soil moisture values in experiment IV and V at -2.5, -19.0, and -35.0 cm depth in the soil column.

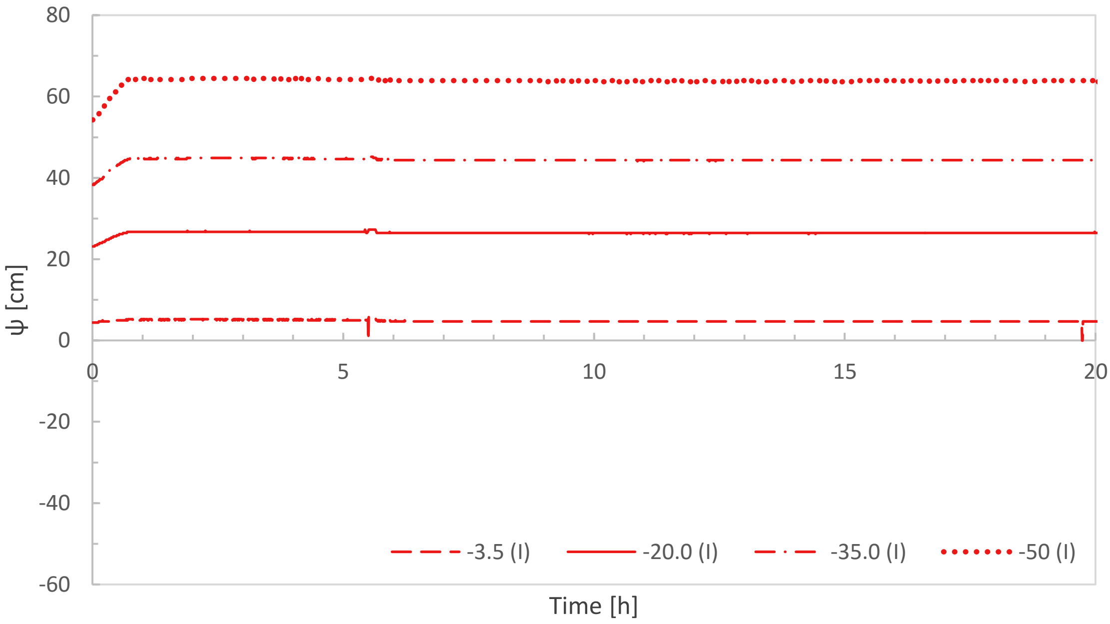

Figure 10-7 Matric potential at -3.5, -20.0, -35.0, and -50.0 cm depth for experiment I. In experiment I, the saturated outflow was measured (with infiltration the bottom) at a total head difference of 12.0 cm. The matric potential remains stable over 20 hours.

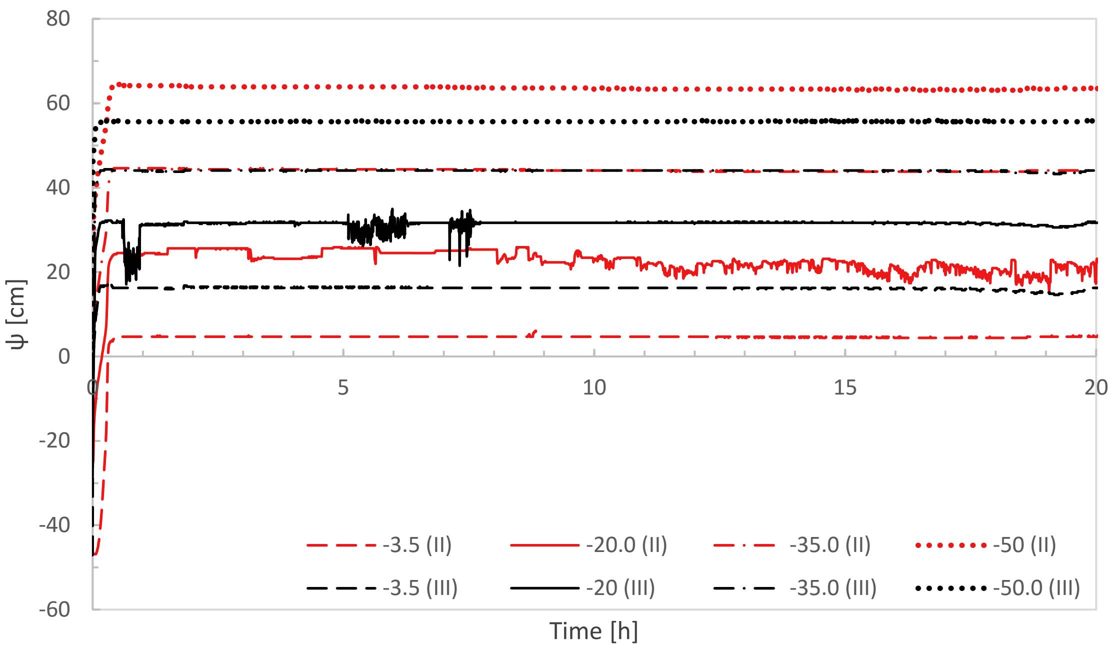

Figure 10-8. The matric potential profiles of experiment II and III after 20 hours. The sensor at -20.0 cm depth did not make good contact to the datalogger, hence the irregular pattern in both experiments. The matric potential is stable over depth and time for both experiments.

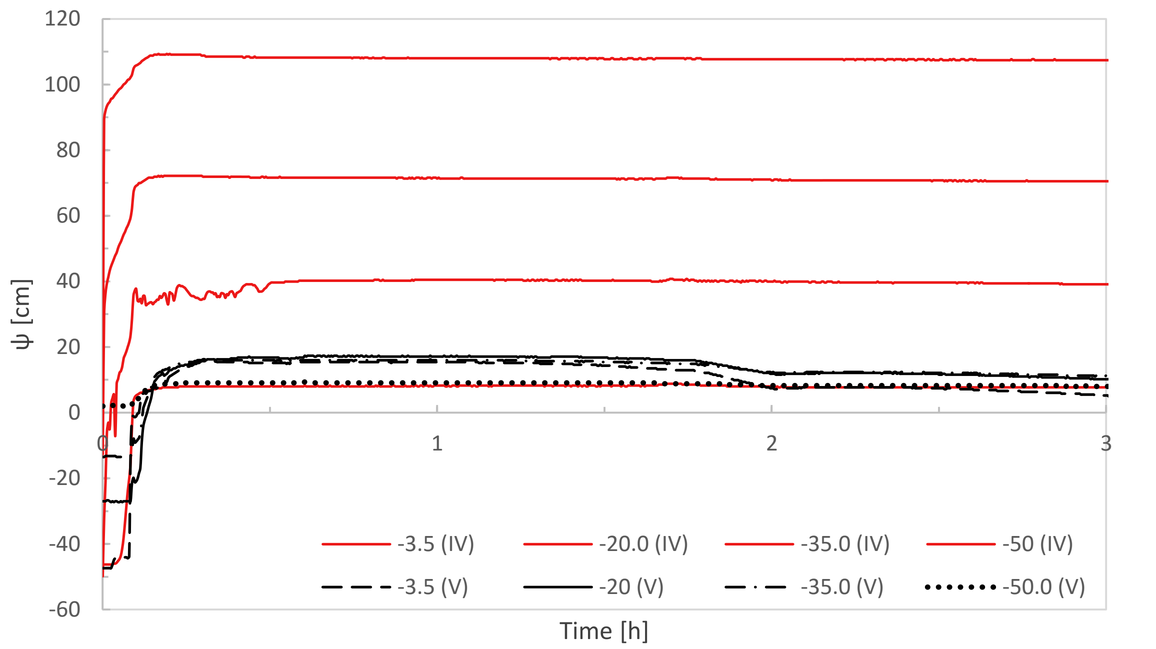

Figure 10-9. The matric potential profiles in experiment IV and V after 3 hours. No data after 3 hours for experiment IV was recorded as it was decided to terminate the experiment when the flux was constant 3 hours after the start of experiment IV.

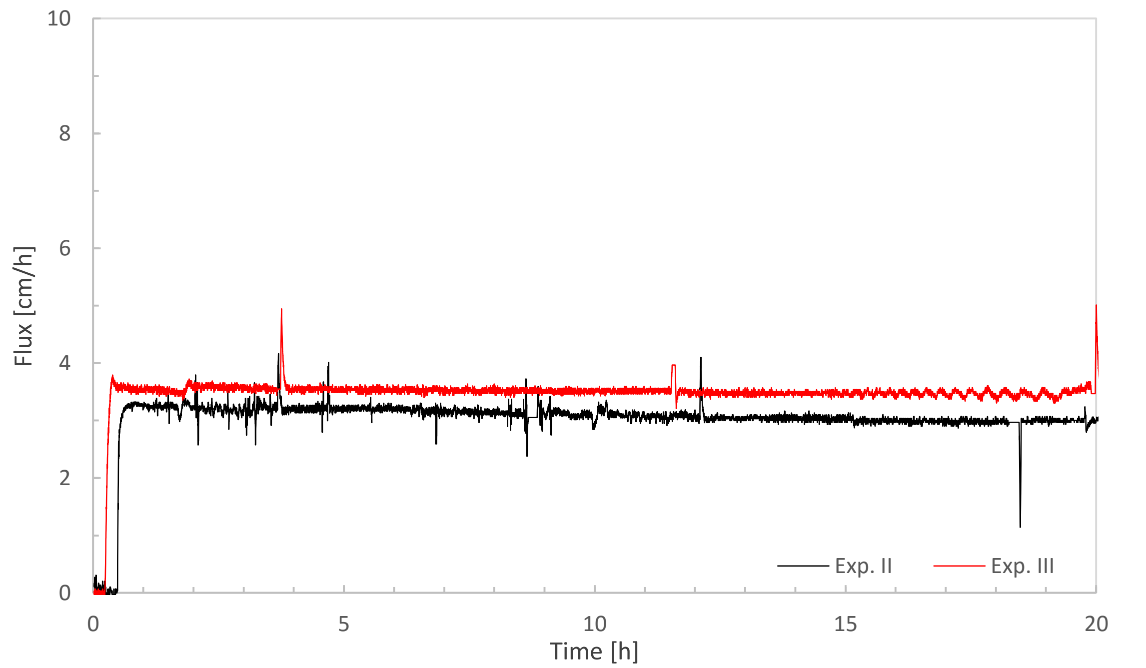

Figure 10-10. Long term flux in experiments II and III.

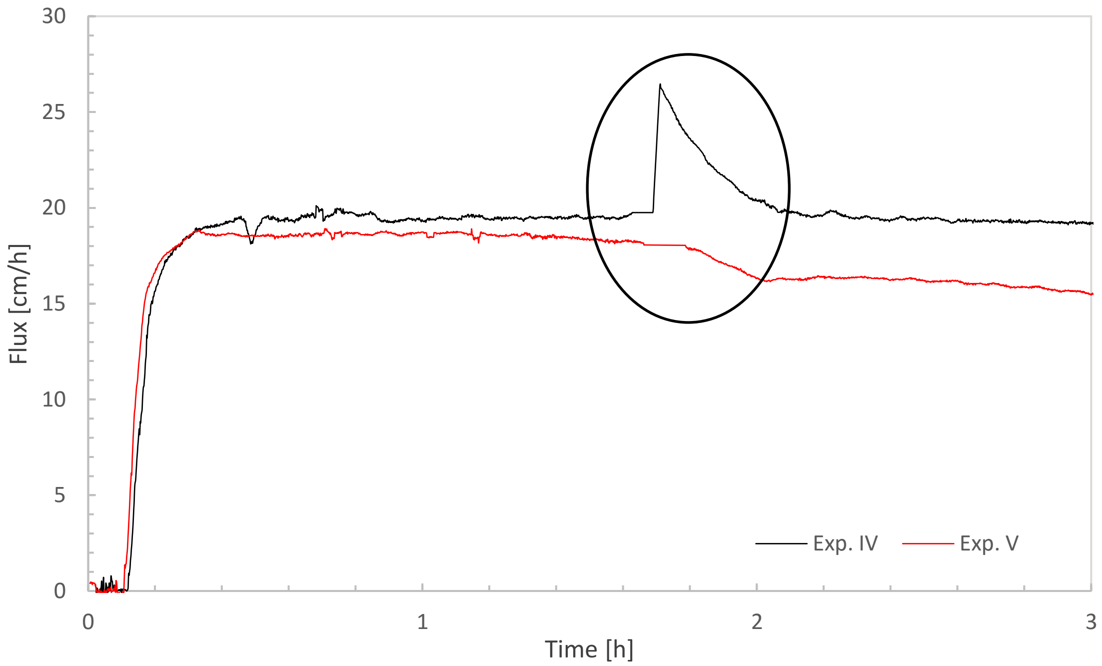

Figure 10-11. Long term flux in experiments IV and V. The circle around the flux in experiment V denotes the loss of the constant ponding head on top of the soil column. The peak in experiment IV is due to closing outflow valve (V5) during emptying of the containers. During this procedure V5 is closed to allow emptying of container A without spilling outflow water. Additionally, the overflow valve OF3 was too small to discharge the build up of water fast enough to retain a constant ponding pressure. As a consequence of this procedure a higher flux results when V5 was opened again.

11 APPENDIX TEXT

11.1 Detailed description of the experiment

Firstly, in section 11.1.1 the procedure for filling up the column with sand is explained, insertion of the sensors, and the procedure for injecting CO_2 into the discharge chamber. After the CO_2 injection the column was slowly saturated (0) to prepare for the first experiment. The experiment was started by obtaining the saturated flux (Experiment I) from which saturated conductivity was determined (11.1.2) to be used in Hydrus 1D and to assess air entrapment. In part 11.1.3, 11.1.4, 11.1.5 and 11.1.6 the goal of the column experiment was to evaluate effects of air entrapment by doing 4 experiments (II, III, IV, and V). The specific procedure of all steps is outlined below as well as a description of the column set up. The table below summarizes the description this experiment and the order of steps.

Table 11-1. An overview of the experiments along with the tables and figures belonging to each experiment.

Part	**Table**	***Figure***	***Comment***
3.1.1	-	Figure 10-2	Column set up/description
0	Table 11-2		Filling column with sand/inserting sensors/CO_2 injection
0	Table 11-3		Slow saturation bottom
	Experiment I (11.1.2)		**Saturated outflow during bottom infiltration (12.0 cm pressure difference).**
11.1.2	Table 11-4		Infiltration at the bottom of the column, 12.5 cm ponding
	Experiment II (11.1.3)		**Infiltration at the bottom of the column, 12.0 cm pressure difference (Outflow through**
11.1.3.1	Table 11-5,Table 11-6		Drain inflow reservoir 1 (IR1) (priming)
11.1.3.2	Table 11-7		Draining column 3.806 days (set initial conditions)
11.1.3.3	Table 11-8		Filling up IR1 until 0.0 cm
11.1.3.4	Table 11-3, Table 11-4		Infiltration bottom, 12.5 cm ponding
	Experiment III (11.1.4)		**Infiltration at the top of the column, 12.0 cm pressure difference (Outflow through V7).**
11.1.4.1	Table 11-5,Table 11-6		Draining IR1 (priming)
11.1.4.2	Table 11-7		Draining column 3.806 days (set initial conditions)
11.1.4.3	Table 11-8		Filling up IR1 until 0.0 cm
11.1.4.4	*Table 11-9*		Infiltration top soil column, 12.5 cm ponding
	Experiment IV (11.1.5)		**Infiltration at the bottom of the column, 62.0 cm pressure difference (Outflow through V5).**
11.1.5.1	Table 11-10		Draining ponding layer soil column
11.1.5.2	Table 11-7		Draining column (set initial conditions)
11.1.5.3	Table 11-8		Filling up IR1 to 50.0 cm
11.1.5.4	Table 11-3*Table 11-9*		Infiltration at the bottom of the column, 62.5 cm ponding.
	Experiment V (11.1.6)		**Infiltration at the top of the column, 62.0 cm pressure difference (outflow through V2).**
11.1.6.1	Table 11-10		Draining IR1 (priming)
11.1.6.2	Table 11-7		Draining column (setting initial conditions)
11.1.6.3	Table 11-8		Filling up IR1 to 0.0 cm
11.1.6.4	Table 11-11		Infiltration at the top of the soil column (12.5 cm ponding)

11.1.1 Packing the column, inserting sensors and removal of air from the discharge chamber.

Packing the column with sand and inserting sensors

The sand of the column is homogenized to prevent occurrence of layers with a different grain size. The column was filled with air dried sand from the dunes at Meijendel. The column was filled by adding a layer of two centimeter each time, then was compacted by applying pressure carefully with a long, heavy, plastic rod with a diameter of about 4.0 cm. The layer of sand is roughened before the next layer is built on top of it. While packing the column, sensors for soil moisture (EC-5) were inserted. The soil moisture sensors are fully embedded in the column, the matric potential were inserted about 10.0 cm horizontally in the sand column after the packing has been done. The added weight for each layer is given in *Table 11-12*.The thickness of the layers may vary slightly as the height of the sand could only be measured at the wall of the column. Also, the added weight can differ due to differences in the water content of the sand. Especially, from layer 20 to 28 the weight of the added sand was more in comparison to the previous layers. This is due to the fact that the sand had not been air dried as long as the sand coming from previous containers. Initially, the sand had a soil moisture content of about 8 to 9 percent.

Removing air from the discharge chamber with CO_2.

Before saturating the column from below, air had to be removed from the discharge chamber and sand column. When starting infiltration of water from below without injecting CO_2, an unnatural amount of air will be pushed through the column by the advancing water front. CO2 will dissolve more easily into water, causing a smaller buildup of gasses ahead of the wetting front. Filling up the sand column, discharge chamber and tubes by injecting CO_2 (through the left cap on the discharge chamber), enables escape of air at the top of the column or through the right cap.
To remove air in the discharge chamber;

- Close V2 and V3 and open V1 (Table 11-2) and let IR1 fill (V6 open) with water until V7 flows over (close V6).
- Shortly open V2 to let any trapped air escape along with the water discharging, then close V2 again.
- Open V5, V7.
- Open the cap on the left hand side of the discharge chamber and pump CO_2 in.
- The remainder of air in the discharge chamber can be removed by opening the cap on the right side as well.
- Degassing ceased after 7 days, 5 hours, 41 minutes (7.24 days).

Variables measured:

Table 11-2 Setting of the valves during CO_2 injection

	Open	Closed		Open	Closed
V1	X		V6		x
V2		x	V7	x	
V3		x			
V4		x			
V5	X				

Saturating the column

To measure saturated outflow the column had to be saturated very slowly from the bottom. The reason to choose for filling up through the bottom is because the infiltration front will be pushed up evenly by the flux from below, which will prevent entrapment of naturally present air in the column.

To conduct this step;

- Open V2 to drain the water in IR1 to prevent the water from entering the column with a high pressure.
- Close V2.
- Open V3 (Table 11-3).
- Open V6 (to turn on the tap), tap velocity was set at 2.5 L/h (comparable to 2.33 cm/h).
- The column is ‘saturated’ when water discharges through the tube at the top of the soil column into container A.
- Empty container A.

Variables measured: Matric potential and soil moisture.

Table 11-3 Setting of the valves during saturation or infiltration from the bottom of the column

	Open	Closed		Open	Closed
V1	X		V6	x	
V2		x	V7		x
V3	X				
V4		x			
V5	x				

11.1.2 Exp I: Saturated outflow during bottom infiltration

To conduct this step;

- Keep the valves in the same configuration as in Table 11-3, but allow the water in IR1 to build up from 0.0 to 12.0 cm height to create a constant pressure boundary.
- When the water height in IR1 is at 12.5 cm and the outflow is constant this part of the experiment is finished.
- Switch off the water tap (close V6) and close V1 (see Table 11-4).
- Empty A, B and C.

Variables measured: Soil moisture, matric potential, outflow.

Table 11-4 Configuration of the valves after infiltration or saturation of the column from below

	Open	Closed		Open	Closed
V1		x	V6		x
V2		x	V7		x
V3	x				
V4		x			
V5		x			

11.1.3 Exp. II: Bottom infiltration with a total head difference of 12.0 cm

In section 11.1.3 (Experiment II), the outflow flux is measured when infiltrating water at the bottom of the column. In order to make the column ready for infiltration at the bottom, the ponding water layer in IR1 (from experiment I) and the column need to be drained first. Draining IR1 (11.1.3.1**)** is necessary to do because when starting infiltration at the bottom the water entering the column must be applied by a constant flux (as stated above) first and then a constant pressure of 72.0 cm. If not draining IR1, the boundary condition will become constant pressure instantly, which does not occur naturally. After drainage of IR1, the column was drained for 3.806 days (11.1.3.2). The maximum level for the water to decrease to is at the artificial water table at -48.5 cm. The water pressure at -48.5 cm will remain 0.0 cm, because at V2 (-48.5 cm) there is atmospheric pressure. Water overflowed at V2 into container A, B and C, until hydrostatic equilibrium was reached. When hydrostatic equilibrium was attained, the water level in IR1 was set at 0.0 cm again by closing V2 and V3 first, then opening V1 and the tap until water flows from V7 (11.1.3.3). Then, the experiment could start by opening V3 and the tap (V6) (11.1.3.4, Experiment II)

11.1.3.1 *Draining IR1 (priming).*

To drain IR1;

- V1 and V6 are closed (see Table 11-5).
- Open V7.
- When no more water drains from IR1, empty A, B and C.
- Close V7 (Table 11-6).

Variables measured: -

Table 11-5. Setting of the valves for draining IR1

x	Open	Closed		Open	Closed
V1		x	V6		x
V2		x	V7	x	
V3	x				
V4		x			
V5	x				

Table 11-6 Configuration of the valves after drainage of IR1.

x	Open	Closed		Open	Closed
V1		x	V6		x
V2		x	V7		x
V3	x				
V4		x			
V5	x				

11.1.3.2 *Draining the sand column (set initial conditions).*

To conduct this step;

- Open V1, and then V2 (Table 11-7).
- When the water level in the tube below IR1 is near -48.5 cm, close V1.
- After 3.806 days close V3.
- Empty container the external reservoir.

Variables measured: soil moisture, matric potential, water height in IR1 with Keller device outflow in container A, B and C.

Table 11-7 Configuration valves when draining the sand column

	Open	Closed			Open	Closed
V1	x			V6		x
V2	x			V7	x	
V3	x					
V4		x				
V5	x					

11.1.3.3 *Filling up IR1 until 0.0 cm*

To conduct this step (see Table 11-8):

- Close V2 and V3
- Open V1 and V6

Variables measured: -

Table 11-8 Configuration of the valves during filling up IR1 to 0.0 cm

	Open	Closed		Open	Closed
V1	x		V6	x	
V2		x	V7	x	
V3		x			
V4		x			
V5	x				

11.1.3.4 *Measuring outflow when infiltrating from the bottom (Experiment II)*

Now infiltration starts by;

- Opening V3 (Table 11-3).
- Close V7
- Opening V6 (open the tap, about 103 L/h, +-95.7 cm.h^{-1})
- When the water level in IR1 is at 12.5 cm, lower the tap velocity accordingly, so that the overflow in IR1 to the external reservoir is minimized.
- Infiltration stops when a constant flux discharges from the top of the sand column into the containers A, B and C.
- Stop the tap (V6), close V1 (Table 11-4).
- Empty A, B and C.

Variables measured: Soil moisture, matric potential, outflow in containers A, B and C, and water level in the external reservoir and IR1.

11.1.4 Exp III: Top infiltration with a total head difference of 12.5 cm.

In 11.1.4 the outflow flux was measured when infiltrating under pressure from above. Before starting infiltration at the top, the column had to be made ready by a few priming steps, and then initial conditions need to be set. In the following section the priming steps and setting of initial conditions are described and it is explained why these steps are necessary. First, draining of IR1 (11.1.4.1) from 12.5 to 0.5 cm was necessary to do because, as said before, when starting infiltration at the bottom or top the water entering the column must be applied by a constant flux first and then a constant pressure of 12.5 cm. After draining IR1, the sand column was drained (11.1.4.2) for 3.806 days. Also, the water level in IR1 was set at 0.0 cm again (11.1.4.3). Then it was followed by infiltration (Experiment III) of water by a constant flux going to constant pressure when the water height at the soil surface has reached a height of 13.0 cm (11.1.4.4). The pressure at the bottom of the column prior to the start of the experiment is +11.0 cm.

11.1.4.1 *Draining IR1 (priming).*

To drain IR1 (see Table 11-5):

- Open V7.
- When no more water drains from IR1, close V7 (Table 11-6).
- Empty the external reservoir.

Variables measured: -

11.1.4.2 *Draining the sand column (set initial conditions).*

To conduct this step;

- Open V1, and then V2 (Table 11-7)
- When the water level in the tube below IR1 is near -48.5 cm, close V1.
- After 3.806 days close V3.
- Empty container A, B and C.

Variables measured: soil moisture, matric potential, water height in IR1 with Keller device outflow in container A, B and C.

11.1.4.3 *Filling up IR1 until 0.0 cm.*

To conduct this step (Table 11-8):

- Close V2 and V3
- Open V1 and V6 until the water level is at 0.0 cm (when water starts to flow through V7)

Variables measured: -

11.1.4.4 *Infiltration at the top, air confining conditions (Experiment III).*

Now water can be infiltrated at the top of the column as follows:

- Put the tap onto the sand column.
- Close V5 (Table 11-9).
- Open the tap (open V6) (tap velocity 103 L.h^{-1}, +-95.7 cm.h^{-1}).
- Open V3.
- When water on top of the sand column has reached a height of 13.0 cm, water will start to overflow into the external reservoir through overflow tube OF1 and the tap velocity can be adjusted accordingly, so that the overflow in the soil column to the external reservoir is minimized.
- Once the outflow in to the containers A, B and C reaches a constant value the experiment the tap can be switched off (close V6).
- Empty A, B and C.

Variables measured: *Soil moisture, matric potential, air pressure and outflow in A, B and C*

Table 11-9 Setting of the valves during infiltration at the top in experiment III

	Open	Closed		Open	Closed
V1	x		V6	x	
V2		x	V7	x	
V3	x				
V4		x			
V5		x			

In the next set of experiments (IV and V) (11.1.5 and 11.1.6) the outflow flux was evaluated again by first infiltrating at the bottom and then at the top of the column. The difference with experiment II and III is that the total head difference between the outflow point and the top of the water layer either on top of the column or in IR1 was 61.5 or 62.9 cm, respectively.

11.1.5 Exp. IV: Bottom infiltration, total head difference: 62.9 cm.

In experiment IV (Figure 3-5) the water layer on top of the column was drained into a separate container, so that the water level in both IR1 as the soil column is at 0.0 cm (11.1.5.1). Then, the column will be drained by opening V2 (11.1.5.2). After 3.806 days of drainage, the water level in IR1 is first set to 50.0 cm (by closing V3)(11.1.5.3) before the experiment can start by quickly increasing the ponding layer in IR1 from 50.0 to 62.5 cm height (11.1.5.4).

11.1.5.1 *Draining the water layer on the soil column).*

To drain (see Table 11-10);

- Open V5.
- Empty the external reservoir when no more water drains from the soil column through V5

Variables measured: -

Table 11-10 Setting of the valves during drainage of the ponding layer on top of the column, through V5.

	Open	Closed		Open	Closed
V1		x	V6		x
V2		x	V7	x	
V3	x				
V4		x			
V5	x				

11.1.5.2 *Draining the sand column (set initial conditions).*

To conduct this step;

- Open V1, and then V2 (Table 11-7).
- When the water level in the tube below IR1 is near -48.5 cm, close V1.
- After 3.806 days close V3.
- Empty container A, B and C.

Variables measured: soil moisture, matric potential, water height in IR1 with Keller device outflow in container A, B and C.

11.1.5.3 *Filling up IR1 until 50.0 cm*

- To conduct this step (*Table 11-8*);
- Put the tap onto IR1.
- Close V2.
- Open V1 and V6 until the water level is at 0.0 cm (when water starts to flow through V7).
- Close V6.

Variables measured: -

11.1.5.4 *Infiltration at the bottom of the column (Experiment IV).*

Now water can be infiltrated at the bottom of the column as follows:

- Close V7 (Table 11-3).
- Open the tap (V6) (tap velocity 103 L.h^{-1}, +-95.7 cm.h^{-1}).
- Open V3.
- When water in IR1 has reached a height of 62.9 cm, water will start to overflow into the external reservoir via overflow tube OF3 and the tap velocity can be adjusted accordingly, so that the overflow in IR1 to the external reservoir is minimized.
- Once the outflow in to the containers A, B and C reaches a constant value the experiment the tap can be switched off (close V6).

Variables measured: *Soil moisture, matric potential, air pressure and outflow in A, B and C.*

11.1.6 Exp.V: Infiltration at the top of the column, total head difference 61.5 cm.

In experiment V, the water layer in IR1 is first drained into a separate container, so that the water level in both IR1 as the soil column is at 0.0 cm (11.1.6.1). Then, the column will be drained by opening V2 (11.1.6.2). After 3.806 days of drainage, the experiment can start by quickly increasing the ponding layer at the top of the soil surface from 0.0 to 13.0 cm height (11.1.6.4). V2 is opened at the moment that the first water infiltrates into the soil. The water will move from the top of the column to the bottom of the column where it can flow out through V2 into container A, B and C.

11.1.6.1 *Draining ponding layer in IR1 (priming).*

To drain the ponding layer on top of the column (Table 11-5):

- Close V1.
- Open V7 and let water drain into external reservoir.
- When no more water drains from IR1, empty the external reservoir.

Variables measured: -

11.1.6.2 *Draining the sand column (set initial conditions).*

To conduct this step;

- Open V1 and then V2 (Table 11-7).
- When the water level in the tube below IR1 is near -48.5 cm, close V1.
- After 3.806 days close V3.
- Empty container A, B and C.

Variables measured: soil moisture, matric potential, water height in IR1 with Keller device and outflow in container A, B and C.

11.1.6.3 *Filling up IR1 until 0.0 cm*

To conduct this step (Table 11-8):

- Close V2.
- Open V1 and V6 until the water level is at 0.0 cm (when water starts to flow through V7).
- Close V6.

Variables measured: -

11.1.6.4 *Experiment V*

Now water can be infiltrated at the top of the column as follows:

- Put the tap onto the sand column.
- Close V5 and V1 (Table 11-11).
- Open the tap (open V6) (tap velocity 103 $L.h^{-1}$, +-95.7 $cm.h^{-1}$).
- Open V3 and V2.
- When water on top of the sand column has reached a height of 12.5 cm, water will start to overflow into the external reservoir via the overflow tube and the tap velocity can be adjusted accordingly, so that the overflow in IR1 to the external reservoir is minimized.
- Once the outflow in to the containers A, B and C reaches a constant value the experiment the tap can be switched off (close V6).

Variables measured: soil moisture, matric potential, water height in IR1 with Keller device and outflow in container A, B and C.

Table 11-11 Setting of the valves during infiltration at the top in experiment V

	Open	Closed		Open	Closed
V1		X	V6	x	
V2	X		V7	x	
V3	x				
V4		x			
V5		x			

Table 11-12. The layers and weight added to the column in each layer. The total bulk density is 1709 kg.m-3.

Layer	Top layer	Bottom layer	Total added sand
[#]	[cm]	[cm]	[g]
1	0.0	-2.0	3155.3
2	-2.0	-4.0	4731.8
3	-4.5	-6.8	3494.9
4	-6.8	-9.0	3347.8
5	-9.0	-11.0	4500.7
6	-11.0	-13.0	3498.9
7	-13.0	-15.0	3496.7
8	-15.0	-17.0	3501.4
9	-17.0	-19.0	3500.1
10	-19.0	-21.0	3499.3
11	-21.0	-23.0	3497.1
12	-23.0	-26.0	5248.3
13	-26.0	-28.0	3494.3
14	-28.0	-30.0	4366.0
15	-30.0	-32.0	3489.8
16	-32.0	-34.0	3495.0
17	-34,0	-36.0	3782.1
18	-36.0	-38.0	4497.8
19	-38,0	-41.5	5245.4
20	-41.5	-43.0	3494.9
21	-43.0	-45.0	3494.4
22	-45.0	-47.0	3996.9
23	-47.0	-49.0	3496.3
24	-49.0	-51.0	4994.9
25	-51.0	-53.0	3997.1
26	-53.0	-55.0	3746.3
27	-55.0	-57.0	3743.8
28	-57.0	-59.2	3996.2

Total added sand	Total added sand	Total volume	Total bulk density
[g]	[kg]	[m^3]	[$kg.m^3$]
108,803.5	108.80	0.0637	1709.3

1156